



doi:10.1016/S0016-7037(03)00266-7

Kinetic and equilibrium Fe isotope fractionation between aqueous Fe(II) and Fe(III)

S. A. WELCH,^{1,†} B. L. BEARD,¹ C. M. JOHNSON,^{1,*} and P. S. BRATERMAN²¹Department of Geology and Geophysics, UW Madison, 1215 West Dayton St., Madison WI 53706 USA²Department of Chemistry, University of North Texas, PO Box 305070, Denton TX 76203 USA

(Received October 28, 2002; accepted in revised form April 11, 2003)

Abstract—Equilibrium and kinetic Fe isotope fractionation between aqueous ferrous and ferric species measured over a range of chloride concentrations (0, 11, 110 mM Cl⁻) and at two temperatures (0 and 22°C) indicate that Fe isotope fractionation is a function of temperature, but independent of chloride contents over the range studied. Using ⁵⁷Fe-enriched tracer experiments the kinetics of isotopic exchange can be fit by a second-order rate equation, or a first-order equation with respect to both ferrous and ferric iron. The exchange is rapid at 22°C, ~60–80% complete within 5 seconds, whereas at 0°C, exchange rates are about an order of magnitude slower. Isotopic exchange rates vary with chloride contents, where ferrous-ferric isotope exchange rates were ~25 to 40% slower in the 11 mM HCl solution compared to the 0 mM Cl⁻ (~10 mM HNO₃) solutions; isotope exchange rates are comparable in the 0 and 110 mM Cl⁻ solutions.

The average measured equilibrium isotope fractionations, Δ_{Fe(III)-Fe(II)}, in 0, 11, and 111 mM Cl⁻ solutions at 22°C are identical within experimental error at +2.76±0.09, +2.87±0.22, and +2.76±0.06 ‰, respectively. This is very similar to the value measured by Johnson et al. (2002a) in dilute HCl solutions. At 0°C, the average measured Δ_{Fe(III)-Fe(II)} fractionations are +3.25±0.38, +3.51±0.14 and +3.56±0.16 ‰ for 0, 11, and 111 mM Cl⁻ solutions. Assessment of the effects of partial re-equilibration on isotope fractionation during species separation suggests that the measured isotope fractionations are on average too low by ~0.20 ‰ and ~0.13 ‰ for the 22°C and 0°C experiments, respectively. Using corrected fractionation factors, we can define the temperature dependence of the isotope fractionation from 0°C to 22°C as:

$$10^3 \ln \alpha_{\text{Fe(III)-Fe(II)}} = \frac{[0.334 \pm 0.032] * 10^6}{T^2} - 0.88 \pm 0.38$$

where the isotopic fractionation is independent of Cl⁻ contents over the range used in these experiments.

These results confirm that the Fe(III)-Fe(II) fractionation is approximately half that predicted from spectroscopic data, and suggests that, at least in moderate Cl⁻ contents, the isotopic fractionation is relatively insensitive to Fe-Cl speciation. Copyright © 2003 Elsevier Ltd

1. INTRODUCTION

The iron isotope composition of most terrestrial igneous rocks is extremely homogenous (δ⁵⁶Fe = 0.00 ± 0.05 ‰), although isotopic variations up to 4–5 ‰ have been observed for Fe-bearing minerals that have been chemically precipitated from solution (e.g., Beard and Johnson, 1999; Zhu et al., 2000; Beard et al., 2002; 2003a; 2003b; Johnson et al., 2003a). The largest isotopic fractionations appear to occur between ferrous and ferric species in inorganic or biologic systems (e.g., Beard et al., 1999; 2003a; Johnson et al., 2002a; 2002b). In general, the lowest δ⁵⁶Fe values are associated with reduced Fe minerals such as siderite and pyrite, whereas ferric oxide phases have higher δ⁵⁶Fe values (Johnson et al., 2003a). Modern Fe-oxyhydroxide accumulations have a range in δ⁵⁶Fe values that is nearly as large as that found in banded iron formations, although without the high positive δ⁵⁶Fe values found in the banded iron formations (e.g., Bullen et al., 2001; Poulson et al., 2002). Significant fractionation (up to 2 ‰) between the dissolved ferrous iron in solution and the precipitated ferric oxyhydroxide phases has been measured in several cases. This large variability in ⁵⁶Fe/⁵⁴Fe ratios may reflect kinetic fraction-

ations during precipitation of Fe phases or, alternatively, equilibrium isotope fractionations between dissolved Fe(II) and Fe(III) species and precipitated Fe minerals. Biologically mediated oxidation or reduction of iron produces a ~+1.3 to +1.5 ‰ fractionation in ⁵⁶Fe/⁵⁴Fe ratios between ferrous and ferric components (Beard et al., 1999; 2003a; Croal et al., 2002).

Interpretation of the iron isotope variability that is preserved in chemical precipitates may be further complicated because the isotopic effects due to speciation of aqueous ferric and ferrous iron solutions is unknown. Isotopic fractionation is expected between metal species that have different bonding environments or coordination (i.e., octahedral vs. tetrahedral), ligand complexation, or redox state, where the heavier isotope would generally be expected to be concentrated in the species that has the stronger bonds (Urey, 1947). Large variations in equilibrium Fe isotope fractionation between different iron species and iron minerals have been predicted from spectroscopic data (Polyakov, 1997; Polyakov and Mineev, 2000; Schauble et al., 2001). For example, Schauble et al. (2001) predict a fractionation of +5.5 ‰ in ⁵⁶Fe/⁵⁴Fe between hexa-aquo ferric and hexa-aquo ferrous iron in solution at room temperature. Additionally, isotopic fractionations between monochloro-substituted ferric iron and hexa-aquo ferrous iron are predicted to be much lower, ~4 ‰, because chloride substitution results in longer (weaker) Fe(III)-ligand bonds. However, the predicted isotopic fractionations are almost twice

* Author to whom correspondence should be addressed (clarkj@geology.wisc.edu).

† Present address: Geology Department/RSES, the Australian National University, Canberra, ACT, 0200 Australia.

that measured in dilute acid chloride solutions (Johnson et al., 2002a) which are interpreted to reflect equilibrium Fe isotope fractionation. Large variations in Fe isotope compositions in other experimental studies have been attributed to fractionation between different dissolved ferrous and/or ferric species (e.g., Anbar et al., 2000; Bullen et al., 2001; Matthews et al., 2001; Zhu et al., 2002). However, it is difficult to establish if these observations reflect equilibrium or kinetic effects, although in the work reported by Matthews et al. (2001), they clearly demonstrated that kinetic isotope effects were present in their experiments.

The purpose of the present experiments was to investigate the effects of chloride complexation and temperature on the equilibrium isotope fractionation and kinetics of isotopic exchange between aqueous ferrous and ferric iron. Experiments were conducted at two temperatures and a range of chloride concentration that spans those that are typical for Earth surface conditions.

2. NOTATION AND METHODS

2.1. Notation

Iron isotope compositions for the equilibrium experiments are expressed using the standard per mil (‰) notation of $\delta^{56}\text{Fe}$ and $\delta^{57}\text{Fe}$ for the $^{56}\text{Fe}/^{54}\text{Fe}$ and $^{57}\text{Fe}/^{54}\text{Fe}$ isotope ratios, respectively, where:

$$\delta^{56}\text{Fe} = \left(\frac{^{56}\text{Fe}/^{54}\text{Fe}_{\text{sample}}}{^{56}\text{Fe}/^{54}\text{Fe}_{\text{igneous rocks}}} - 1 \right) * 1000 \quad (1)$$

$$\delta^{57}\text{Fe} = \left(\frac{^{57}\text{Fe}/^{54}\text{Fe}_{\text{sample}}}{^{57}\text{Fe}/^{54}\text{Fe}_{\text{igneous rocks}}} - 1 \right) * 1000 \quad (2)$$

Iron isotope composition for the kinetic experiments, which use ferric solutions enriched in ^{57}Fe , are expressed in terms of $\delta^{57/56}\text{Fe}$ where:

$$\delta^{57/56}\text{Fe} = \left(\frac{^{57}\text{Fe}/^{56}\text{Fe}_{\text{sample}}}{^{57}\text{Fe}/^{56}\text{Fe}_{\text{igneous rocks}}} - 1 \right) * 1000 \quad (3)$$

The reference ratio $^x\text{Fe}/^y\text{Fe}_{\text{igneous rocks}}$ is the average iron isotope composition of 46 igneous rocks ($\delta^{56}\text{Fe} = 0.00 \pm 0.05\text{‰}$) (Beard and Johnson, 1999; Beard et al., 2003a). Using the iron isotope composition of average igneous rocks, as opposed to choosing an arbitrary pure metal standard, follows the approach of other stable isotope systems such as oxygen, which reference isotope values relative to a significant planetary reservoir such as Standard Mean Ocean Water. On this scale, the $\delta^{56}\text{Fe}$ and $\delta^{57}\text{Fe}$ values of isotope standard IRMM-014 are $-0.09 \pm 0.05\text{‰}$ and $-0.11 \pm 0.07\text{‰}$ (1σ , $n = 49$) respectively. Fractionation in Fe isotope compositions between coexisting ferric and ferrous species is expressed as:

$$\Delta_{\text{Fe(III)-Fe(II)}} = \delta^{56}\text{Fe}_{\text{Fe(III)}} - \delta^{56}\text{Fe}_{\text{Fe(II)}} \approx 10^3 \ln \alpha_{\text{Fe(III)-Fe(II)}} \quad (4)$$

2.2. Experimental Design

Experiments were conducted to determine the effects of iron-chloride speciation on the kinetics of the ferrous-ferric

exchange reaction and the equilibrium isotopic fractionation between ferrous and ferric iron in solution. The kinetics of isotopic exchange were determined using ^{57}Fe -enriched tracer experiments over the same range of Cl^- concentration and temperatures as were studied for the equilibrium experiments. Equilibrium isotopic fractionation between aqueous ferrous and ferric iron was determined using “isotopically normal” iron solutions. A summary of experiments and experimental conditions is listed in Table 1.

Equilibrium isotope fractionation between Fe(II) and Fe(III) species in solution can be determined if the rate of isotopic exchange is relatively slow compared to the rate of separation of the two species. In these experiments, Fe(II) and Fe(III) were separated by a BaCO_3 coprecipitation technique that was modified from that used by Johnson et al. (2002a). For this technique, excess carbonate addition increases solution pH and forces the rapid ($<1-2$ second) precipitation and flocculation of aqueous Fe(III) as iron oxyhydroxides. The rapid and essentially complete separation allows us to “quench in” the isotopic composition of ferrous and ferric in solution. The rise in pH is limited by the hydrogen carbonate - carbonic acid buffer system, and the solid carbonate surface assists nucleation and aggregation of the Fe(III) hydrous oxide. Both these effects will minimize the exchange between Fe(II) and Fe(III) during precipitation. The co-precipitation method was tested with several different bases (SrCO_3 , NH_4OH , and BaCO_3), over a range of Fe(II):Fe_{total} proportions and Fe_{total} concentrations. The most consistent quantitative yields are produced using BaCO_3 ; CaCO_3 was not used because of the potential isobaric interference of $^{40}\text{Ca}^{16}\text{O}$ and $^{40}\text{Ca}^{16}\text{OH}$ on ^{56}Fe and ^{57}Fe , respectively (Johnson et al., 2002a). Both ferrous and total iron were initially measured in the recovered ferrous and ferric phases to determine that ferrous and ferric iron were quantitatively separated by this method.

Kinetic isotope exchange experiments were conducted with ferric solutions enriched in ^{57}Fe and ferrous solutions that had “normal” Fe isotope compositions to determine the kinetics of the ferrous-ferric exchange reaction. Because the initial isotopic contrast between ferric and ferrous components is much greater than that of any equilibrium or kinetic isotopic fractionation, use of enriched tracers allows assessment of the kinetics of isotope exchange that is insensitive to the intrinsic isotopic fractionation between species or components. A disadvantage of using enriched tracers is that small amounts of contamination of ferric Fe in the ferrous aliquot, or vice versa, can significantly change the $\delta^{57/56}\text{Fe}$ values.

For the ^{57}Fe -enriched kinetic experiments conducted at 22°C , 5 mL aliquots of ~ 20 ppm normal ($\delta^{57/56}\text{Fe} = \sim -1\text{‰}$) Fe(II) solutions and ^{57}Fe spiked ($\delta^{57/56}\text{Fe} = \sim +331\text{‰}$) Fe(III) solutions (see Table 1) were pipetted directly into a clean polyethylene syringe fitted with a $0.2\ \mu\text{m}$ Luer lock filter and allowed to react for 5 to 120 seconds. Solutions for the 300 second experiments were initially pipetted to a clean centrifuge tube and decanted after ~ 4 min to the syringes. A 0.5 mL suspension of BaCO_3 (50 mg/mL) was added and the solution was immediately (within 2–5 seconds) filtered to separate the aqueous ferrous iron from the ferric precipitates. The ferric precipitates appear to form instantaneously (<1 s). The precipitate is rinsed with an additional 2 mL of water to remove any interstitial ferrous iron. The experiments conducted at 0°C were

Table 1. Summary of experiments conducted.

Kinetics experiments				
Purpose:	Determine the kinetics of the ferrous-ferric isotopic exchange reaction over a range of temperature and chloride concentration			
Method:	Mix aliquots of ~20 ppm ferrous solutions and ~20 ppm ⁵⁷ Fe enriched ferric solutions for 5 to 300 seconds and separate by BaCO ₃ co-precipitation			
Name	Temp	Cl ⁻ mM	Fe(II)/Fe _{total}	Fe solutions*
HNO ₃	22°C	0	0.5	Fe(II)0 and J-M Fe + ⁵⁷ Fe spike in ~10 mM in HNO ₃
HNO ₃ 0°C	0°C	0	0.5	
HCl	22°C	11	0.5	Fe(II)Cl ₂ and J-M Fe + ⁵⁷ Fe spike in ~10 mM in HCl
HCl 0°C	0°C	11	0.5	
LiCl	22°C	110	0.5	Fe(II)Cl ₂ and J-M Fe + ⁵⁷ Fe spike in ~10 mM in HCl + 100 mM LiCl
LiCl 0°C	0°C	110	0.5	
Equilibrium Experiments				
Purpose	Determine the equilibrium fractionation between aqueous ferrous and ferric iron over a range of temperature (0 and 22°C) and Cl ⁻ concentration (0, ~11, and ~111 mM).			
Method	Mix aliquots of ~20 ppm ferrous and ferric solutions and allow to react for several hours before separation by BaCO ₃ co-precipitation.			
Name	Temp	Cl ⁻ mM	Fe(II)/Fe _{total}	Fe solution*
HNO ₃	22°C	0	0.21, 0.51, 0.52, 0.81	Fe(II) from either partially dissolved Fe(II)O or synthetic fayalite. Fe(III)(NO ₃) ₃
HNO ₃ 0°C	0°C	0	0.21, 0.52, 0.81	
HCl	22°C	10.8–11.2	0.19, 0.20, 0.49, 0.79, 0.80	Fe(II)Cl ₂ and Fe(III)Cl ₃
HCl 0°C	0°C	10.8–11.2	0.19, 0.48, 0.79, 0.80	
LiCl	22°C	110.8–111.2	0.19, 0.48, 0.79	Fe(II)Cl ₂ and Fe(III)Cl ₃ with 100 mM LiCl
LiCl 0°C	0°C	110.8–111.2	0.19, 0.48, 0.79	

* Stock solutions, 0.1 M concentration of ferrous and ferric chloride and ferric nitrate, were prepared by dissolving the iron salts in 100 ml of dilute (~1%) hydrochloric or nitric acid. Stock solutions were diluted to approximately 20 mg/l Fe in 10 mM (pH ~ 2.0) hydrochloric or nitric acid to make 500 ml working solutions. The high chloride solutions contained 100 mM LiCl (~111 mM total Cl). The ferrous nitrate solutions were prepared by dissolving either synthetic fayalite (obtained from Dr. Hank Westrich, Sandia National Laboratory) or FeO in dilute (~10 mM) nitric acid for several days. The supernatant was then decanted from the solid phase and diluted to ~20 ppm Fe. Prior to use of the iron solutions, Fe(II) and total Fe contents were measured by ferrozine to ensure that the working solutions had neither oxidized or reduced. All working solutions were purged with N₂ for approximately 10 minutes before use to minimize O₂ content and ferrous iron oxidation.

similar, except that the 20 ppm Fe working solutions were placed in a 0°C ice-water bath for several hours, and syringes and filters were placed in ice to minimize changes in temperature during the seconds to minutes required to complete the experiments.

The experimental procedure was modified slightly for the equilibrium experiments. Aliquots of ~20 ppm ferrous and ferric working solutions were pipetted to acid-washed polypropylene centrifuge tubes to produce a 10 mL total volume that had ferrous to total iron ratios of approximately 0.2, 0.5, or 0.8. Changes in the Fe(II)/Fe_{total} ratio for the equilibrium fractionation experiments provide a robust test of internal isotopic mass balance because issues such as incomplete recovery or partial re-equilibration during separation produce different effects depending upon the ferrous and ferric proportions in solution; these effects are discussed below. Solutions were allowed to equilibrate for several hours to several days either at room temperature or in a 0°C ice bath. Analyses of the ferrous-ferric mixtures before separation showed no measurable change in the Fe(II):Fe(III) ratio while the solutions were allowed to isotopically equilibrate. The 10 mL Fe(II)+Fe(III) mixture was decanted to a clean 10 mL polyethylene syringe before addition

of the BaCO₃ suspension and separation of the ferrous and ferric components.

The iron oxyhydroxide and BaCO₃ precipitates are dissolved by slowly passing 5 mL of 5% HNO₃ followed by 5 mL HNO₃ solution (pH 2) through the filter. After separation, the total iron in the filtrate and the precipitate were measured by the colorimetric *Ferrozine* method (see Stookey, 1970). Experiments where percent recoveries of Fe in the ferrous and ferric separates were within ~100 ± 10% were processed for isotopic analyses. Some samples with poorer recovery in either the ferrous or ferric fraction were also processed for isotopic analyses and the measured δ⁵⁶Fe values were corrected for incomplete recovery of Fe (see discussion below).

2.3. Column Chemistry

All samples were purified by ion-exchange chromatography. Samples were evaporated to dryness several times in 7 mol/L HCl or 8 mol/L HNO₃ + H₂O₂ to ensure that all iron was oxidized. For the ⁵⁷Fe-enriched kinetic experiments, iron solutions were initially purified using cation exchange resin (Bio-Rad AG50W×8, 200–400 mesh, H⁺ form) to separate Fe from

Ba. The Fe solution was evaporated to dryness, dissolved in 7 mol/L HCl, and subsequently passed through miniaturized anion exchange columns (BioRad AG1×4 200–400 mesh, Cl[−] form). For the isotopically “normal” equilibrium experiments, Fe samples were dissolved in 7 mol/L HCl. This procedure produces BaCl₂ precipitates that are insoluble in 7M HCl. The yellow, Fe-bearing solution was separated from the BaCl₂ precipitates by centrifugation. The precipitate was then leached several times with 7 mol/L HCl to remove any residual Fe. In all cases, Fe contents in the residual BaCl₂ precipitates were below detection limits. All supernatants were combined and the Fe solution was passed through large-volume anion-exchange columns (see Beard et al., 2003a, and Skulan et al., 2002 for details) to separate the Fe from any remaining Ba. Samples were passed through a miniaturized version of the anion-exchange columns a second time. The anion exchange chemistry has been extensively tested in our laboratory to ensure that these ion exchange techniques do not bias the iron isotope compositions (e.g., Beard et al., 2003a). After purification by column chemistry, the iron solutions were dried down several times in nitric acid to remove any residual Cl[−] and then diluted to 25 ppm Fe in 2% *Optima* HNO₃.

2.4. Mass Spectrometry Methods

Iron isotopes were measured using a Micromass *IsoProbe*, a multi-collector, inductively-coupled plasma-mass spectrometer (MC-ICP-MS) that includes a hexapole collision cell. The collision-cell produces high sensitivity and eliminates a number of argon isobars from the Fe mass spectrum (e.g., ⁴⁰Ar¹⁴N on ⁵⁴Fe, and ⁴⁰Ar¹⁶O on ⁵⁶Fe). Instrumental mass bias was corrected using a standard-sample-standard approach. Based on long-term reproducibility of standards and duplicate analysis of a wide variety of natural samples, the precision on our iron isotope measurements for ⁵⁶Fe/⁵⁴Fe ratio is ± 0.05 ‰ (1 SD external reproducibility). Over a one-year period, analysis of three Fe solution standards gave the following values: UW J-M Fe δ⁵⁶Fe = +0.25 ± 0.05 ‰, δ⁵⁷Fe = +0.38 ± 0.07 ‰ (n = 47); UW HPS δ⁵⁶Fe = +0.49 ± 0.05 ‰, δ⁵⁷Fe = +0.73 ± 0.07 ‰ (n = 52); IRMM-14 δ⁵⁶Fe = −0.09 ± 0.05 ‰, δ⁵⁷Fe = −0.12 ± 0.07 ‰ (n = 54). Details of the mass spectrometry methods are described in Beard et al. (2003a) and Skulan et al. (2002).

3. RESULTS

We first discuss the recovery and speciation of iron in our experiments, because this information is pertinent to understanding results of both the kinetic and equilibrium experiments. The kinetics of isotopic exchange is then discussed, which provides rate information that determines the time required to attain isotopic equilibrium, and allows us to correct for the small extent of isotopic exchange that occurs during separation of ferrous and ferric iron species in solution. Finally, the experiments conducted using isotopically normal ferrous and ferric Fe are discussed to determine the effect of iron-chloride complexation on the equilibrium isotopic fractionation between ferrous and ferric species in solution, as well as the effect of temperature on the isotopic fractionation factor.

3.1. Iron Recovery

Nominal recovery of ferrous and ferric Fe after separation in the kinetic and equilibrium experiments was generally between 80 and 120% based on *Ferrozine* analysis of the total iron in solution. Experiments with Fe recovery between ~90% and ~110% were selected for isotopic analyses, although some samples with larger errors in recovery in either the ferrous or ferric component were also processed. In general, we observed better separation and recovery of ferrous and ferric Fe for chloride-containing solutions than for the chloride-free experiments at both 0 and 22°C. In the room-temperature experiments (22°C), when Fe recovery was incomplete, it was generally due to a loss of the ferrous component into the ferric oxyhydroxide precipitates. Tests of the Fe recovery using the *Ferrozine* method for both reduced and total Fe for co-precipitation with ferrous iron solutions showed that when ferrous iron was lost into the ‘ferric’ fraction, it was predominately oxidized, indicating that by mass action, ferrous iron was oxidized and precipitated as ferric oxyhydroxides, and not as siderite, which might have been produced when carbonate was added. It is possible that the ferric component could also have passed through the filter either as dissolved monomeric Fe³⁺ or as colloidal Fe(III) oxyhydroxides, which would be recovered in the ‘ferrous’ fraction. Using BaCO₃ as the base as opposed to SrCO₃ or NH₄OH tended to produce a better recovery of Fe(III) phases based on mass-balance determinations using *Ferrozine*. Although the reddish precipitates were observed to form almost instantly upon addition of SrCO₃ and NH₄OH, quantitative recovery of Fe(III) as Fe-oxyhydroxides on the filter was poor, presumably due to the formation of colloidal Fe that was too fine to be removed by the filter. Although CaCO₃ is very effective for co-precipitating ferric iron (see Johnson et al., 2002a), even very small amounts (ppb levels) of Ca may form CaOH⁺ in the plasma and can affect the ⁵⁷Fe measurements. In the low-temperature experiments, nominal Fe recovery of the ferrous component tended to exceed 100%, indicating incomplete removal of the ferric oxyhydroxides. This is not surprising because the kinetics of precipitation and flocculation should be slower at the lower temperature (although the kinetics of isotopic exchange is still slower).

Several sets of experiments were carried out at 50°C. However, in all of these experiments, the bulk of the ferrous iron was rapidly oxidized and precipitated as ferric oxyhydroxides upon addition of BaCO₃, despite the fact that the solutions were purged for several minutes with N₂ gas to reduce dissolved oxygen. None of these samples were processed for isotopic analysis.

3.2. Iron Speciation

The speciation of ferrous and ferric iron in our solutions that existed before separation was calculated using three databases, PHREEQC, WATEQ4F, and MINTeq (Parkhurst, 1995) (see Table 2, Fig. 1). All databases yielded very similar results for Fe speciation (see also Johnson et al., 2002a). Ferrous Fe speciation is dominated by the [Fe^{II}(H₂O)₆]²⁺ complex in all of our experiments. Calculations show that the mono-chloro iron complex, [Fe^{II}Cl(H₂O)₅]⁺, comprises at most 6% of the total ferrous iron in the highest Cl[−] experiments (LiCl-bearing). The

Table 2. Fe(II) and Fe(III) speciation calculations using PHREEQ, WATEQ and MINTEQ (Parkhurst, 1995) for mixtures of the starting solutions used in the kinetic and equilibrium experiments. Percent speciation is calculated based on either total ferrous or ferric iron.

	(mM)		% Fe(II)			%Fe(III)					
	Cl ⁻	Fe(II)	Fe(III)	Fe ²⁺	FeCl ⁺	Fe(OH) ⁺	Fe ⁺³	Fe(OH) ²⁺	FeCl ²⁺	Fe(OH) ₂ ⁺	FeCl ₂ ⁺
22°C data											
Speciation calculations using PHREEQ											
0	0.18	0.18	100.0	0.0	0.0	64.2	34.5	0.0	1.0	0.0	0.0
11	0.18	0.18	99.0	1.0	0.0	59.1	28.1	11.5	0.8	0.4	0.4
111	0.18	0.18	94.9	5.5	0.0	36.5	12.4	43.5	0.2	7.6	7.6
0	0.072	0.286	100.0	0.0	0.0	64.2	34.4	0.0	1.0	0.0	0.0
11.2	0.072	0.286	99.0	1.0	0.0	59.0	28.0	11.7	0.7	0.4	0.4
111.2	0.072	0.286	94.9	5.5	0.0	36.5	12.3	43.6	0.2	7.6	7.6
0	0.286	0.072	100.0	0.0	0.0	64.3	34.6	0.0	1.0	0.0	0.0
10.8	0.286	0.072	99.0	1.0	0.0	59.2	28.3	11.4	0.8	0.4	0.4
110.8	0.286	0.072	94.9	5.5	0.0	36.6	12.4	43.6	0.2	7.6	7.6
0°C data											
0	0.18	0.18	100.0	0.0	0.0	90.6	9.4	0.0	0.1	0.0	0.0
11	0.18	0.18	99.1	1.0	0.0	83.5	8.6	7.2	0.1	0.5	0.5
111	0.18	0.18	94.8	5.7	0.0	54.8	4.1	29.3	0.0	12.2	12.2
22°C data											
Speciation calculations using WATEQ											
0	0.18	0.18	100.0	0.0	0.0	69.7	29.3	0.0	0.8	0.0	0.0
11	0.18	0.18	99.0	1.0	0.0	62.1	26.1	10.7	0.7	0.3	0.3
111	0.18	0.18	95.3	5.2	0.0	49.1	9.9	35.0	0.2	6.1	6.1
22°C data											
Speciation calculations using MINTEQ											
0	0.18	0.18	100.0	0.0	0.0	67.2	31.7	0.0	0.9	0.0	0.0
11	0.18	0.18	100.0	0.0	0.0	59.3	27.9	11.4	0.8	0.4	0.4
111	0.18	0.18	100.0	0.0	0.0	36.9	12.4	43.2	0.2	7.5	7.5

concentration of other ferrous species are negligible, <0.1%. Ferrous speciation at 0°C is similar to that calculated at 22°C.

Speciation of ferric iron is more complicated. At 22°C in the HNO₃ solutions, the speciation is dominated by the

hexa-aquo Fe complex [Fe^{III}(H₂O)₆]³⁺ and the deprotonated [Fe^{III}(H₂O)₅(OH)]²⁺ complex. Fe(III)-nitrate complexes are not predicted by the geochemical models and have not been detected in Fe-nitrate solutions in spectroscopic studies, reflecting the fact that nitrate is an extremely weak ligand (Kanno and Hiraishi, 1982). In the HCl and LiCl solutions, octahedral ferric-chloride complexes comprise approximately 12 and 50% of the total ferric iron, respectively. It is expected under our experimental conditions that essentially all Fe is octahedrally coordinated, although tetrahedrally coordinated Fe(III)-chloride complexes have been detected by several spectroscopic methods for extremely acidic, high-chloride solutions (>1 mol/L HCl) that greatly exceed those of our experiments (e.g., Brady et al., 1964; Sharma, 1974; Sharma et al., 1975; Magini and Radnai, 1979; Kanno and Hiraishi 1982). At 0°C, the deprotonated ferric-hydroxyl and ferric-chloro complexes comprise a smaller percentage of the total ferric iron than at 22°C.

3.3. Isotope Fractionation Results

The kinetics of aqueous ferrous-ferric isotopic exchange, and the equilibrium fractionation between dissolved ferrous and ferric iron, were determined at two temperatures (~0 and 22°C) and a range of Cl⁻ concentrations (0, 11, and 110 mM) (see Table 1). We first focus on the kinetics of ferrous-ferric exchange because the rates of exchange allow us to constrain the time required to attain isotopic equilibrium, as well as the errors associated with partial re-equilibration of ferrous and ferric iron species during precipitation and separation.

3.3.1. Kinetic isotope experiments

The kinetics of Fe isotope exchange were measured using ⁵⁷Fe-enriched tracers, where the initial δ^{57/56}Fe of the Fe(III)

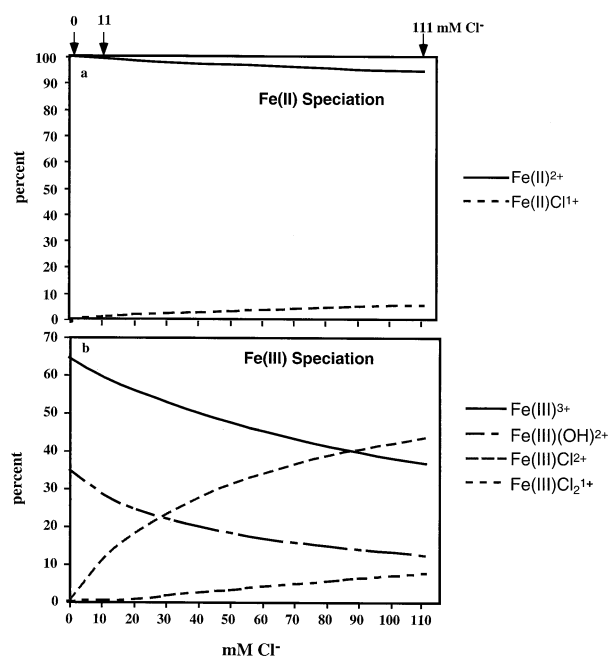


Fig. 1. Plot of (a) ferrous and (b) ferric speciation that spans the range used in the experiments calculated as a function of chloride concentration. Calculations made using PHREEQC (Parkhurst, 1995) for 10 ppm Fe(II) and Fe(III) at pH 2.05 and room temperature). Arrows at 0, 11, and ~111 mM chloride denotes approximate chloride concentrations for HNO₃, HCl, and LiCl experiments.

Table 3. Data for Kinetic ferrous-ferric exchange experiments using ^{57}Fe -enriched tracers at 22°C and 0°C.

Time ^a sec	Fe(II) ^b % rec	Fe(III) ^b % rec	Fe(II) ^c $\delta^{57/56}\text{Fe}$	Fe(III) ^c $\delta^{57/56}\text{Fe}$	Fe(II) ^d F	Fe(III) ^d F	Corrected for partial re-equilibration ^g			
							Fe(II) ^e $\delta^{57/56}\text{Fe}$	Fe(III) ^e $\delta^{57/56}\text{Fe}$	Fe(II) ^f F	Fe(III) ^f F
HNO ₃ experiment at 22°C										
init			-0.9	330.8						
5	93	105	133.1	190.9	0.799	0.851	111.1	215.8*	0.666	0.699*
10	92	111	138.8	190.1	0.833	0.856	118.1	216.6*	0.708	0.695*
30	84	107	157.4	162.7	0.945	1.023	155.3	165.1*	0.933	1.008*
30	93	117	159.0	172.4	0.955	0.963	153.3	180.5*	0.920	0.914*
60	94	111	169.4	164.7	1.018	1.011	171.2	162.3*	1.029	1.025*
60	99	103	169.1	163.9	1.016	1.016	171.0	161.8*	1.028	1.028*
120	94	110	171.7	162.9	1.032	1.021	175.3	158.5*	1.053	1.048*
300	89	114	165.8	167.2	0.996	0.995	165.2	168.0*	0.992	0.991*
HCl experiment 22°C										
init			-1.2	330.3						
5	105	96	104.5	228.4	0.635	0.618	81.5	246.3*	0.497	0.509*
5	101	101	107.5	222.0	0.653	0.656	85.0	245.9*	0.518	0.512*
10	103	101	124.3	205.3	0.754	0.757	108.4	222.3*	0.658	0.654*
10	95	106	126.5	198.1	0.767	0.801	111.7	217.4*	0.678	0.684*
30	95	106	143.6	183.9	0.870	0.887	135.3	194.8*	0.820	0.821*
30	97	106	139.8	189.0	0.847	0.856	129.7	201.9*	0.786	0.778*
60	98	101	159.4	171.2	0.965	0.964	157.0	173.7*	0.951	0.949*
60	101	103	156.5	171.0	0.947	0.965	153.5	174.4*	0.930	0.945*
120	100	105	164.6	166.9	0.996	0.990	164.2	167.5*	0.993	0.987*
120	99	103	164.4	166.7	0.995	0.992	164.0	167.2*	0.992	0.988*
300	98	104	164.4	166.4	0.995	0.994	164.0	166.8*	0.992	0.991*
300	98	102	164.3	165.6	0.994	0.998	164.1	165.9*	0.993	0.996*
LiCl experiment at 22°C										
init			-0.8	331.2						
5	98	103	145.4	191.1	0.847	0.877	131.3	203.4*	0.765	0.800*
5	94	105	145.1	189.2	0.846	0.889	130.7	202.3*	0.762	0.807*
10	105	98	142.3	199.2	0.829	0.826	126.5	212.2*	0.738	0.745*
10	95	106	149.1	188.5	0.869	0.893	137.0	201.0*	0.799	0.815*
30	98	106	160.3	180.8	0.934	0.942	154.1	187.4*	0.898	0.900*
30	101	103	158.6	181.8	0.924	0.935	151.5	188.4*	0.883	0.894*
60	101	107	169.0	173.7	0.984	0.987	167.6	175.2*	0.976	0.977*
60	96	101	170.8	173.1	0.995	0.990	170.3	173.8*	0.992	0.986*
120	95	109	170.8	172.3	0.994	0.995	170.2	172.9*	0.991	0.991*
120	100	109	170.4	172.3	0.992	0.995	169.7	172.9*	0.988	0.991*
HNO ₃ experiment at 0°C										
init			-0.9	330.8						
5	92	85	117.6	195.7	0.705	0.822	114.4	186.9*	0.685	0.875*
10	108	115	148.5	181.2	0.892	0.910	146.7	187.9*	0.881	0.869*
30	105	107	129.8	231.6	0.779	0.604	124.4	243.6*	0.746	0.530*
30	98	101	130.2	229.0	0.781	0.619	125.3	235.1*	0.752	0.582*
60	103	96	126.3	211.2	0.758	0.728	122.3	212.3*	0.733	0.721*
120	95	109	137.8	188.1	0.827	0.868	135.1	195.5*	0.810	0.823*
120	97	105	138.3	190.9	0.830	0.851	135.6	196.2*	0.814	0.819*
300	93	113	153.5	177.5	0.922	0.932	152.1	182.0*	0.914	0.905*
HCl experiment at 0°C										
init			-1.2	330.3						
5	106	102	88.1	243.1	0.536	0.528	82.3	249.0	0.501	0.493
10	100	99	116.3	211.0	0.706	0.723	112.8	214.5	0.685	0.702
30	110	96	96.7	241.4	0.588	0.539	91.2	246.8	0.555	0.506
60	95	108	125.0	182.4	0.758	0.896	122.8	184.5	0.745	0.883
120	99	103	126.8	201.0	0.769	0.783	124.0	203.8	0.752	0.766
120	101	104	131.4	195.9	0.796	0.815	129.0	198.3	0.782	0.800
300	103	99	149.8	203.1	0.907	0.771	147.8	205.1	0.895	0.759
LiCl experiment at 0°C										
Init			-0.8	331.2						
5	99	104	115.4	208.6	0.674	0.767	107.0	214.1	0.625	0.733
10	106	97	105.4	232.9	0.616	0.615	95.5	242.1	0.558	0.557
30	98	100	111.2	223.9	0.649	0.672	102.2	231.7	0.597	0.623
30	99	101	132.9	205.1	0.775	0.789	127.2	210.1	0.742	0.758

Table 3. (Continued)

Time ^a sec	Fe(II) ^b % rec	Fe(III) ^b % rec	Fe(II) ^c $\delta^{57/56}\text{Fe}$	Fe(III) ^c $\delta^{57/56}\text{Fe}$	Fe(II) ^d F	Fe(III) ^d F	Corrected for partial re-equilibration ^g			
							Fe(II) ^e $\delta^{57/56}\text{Fe}$	Fe(III) ^e $\delta^{57/56}\text{Fe}$	Fe(II) ^f F	Fe(III) ^f F
60	97	105	136.4	203.5	0.795	0.800	131.1	208.2	0.765	0.770
60	94	99	138.2	202.8	0.806	0.804	133.2	207.5	0.777	0.774
120	106	96	154.5	192.5	0.900	0.868	152.0	195.6	0.886	0.849
120	98	103	155.0	188.5	0.903	0.894	152.5	191.0	0.889	0.878
300	98	102	165.9	177.7	0.966	0.961	165.0	178.6	0.961	0.955
300	100	101	165.2	175.4	0.962	0.976	164.2	175.9	0.956	0.972

^a Time since ferrous and ferric solutions were mixed.

^b Percent Fe recovered after separation of ferrous-ferric mixture.

^c Measured $\delta^{57/56}\text{Fe}$ for recovered ferrous and ferric fractions.

^d F values calculated for ferrous and ferric fractions. $F = (\delta - \delta_i)/(\delta_e - \delta_i)$. Equilibrium values (δ_e) for experiments were determined from the measured $\delta^{57/56}\text{Fe}$ of 50:50 mixture of the starting solutions and are 166.4, 165.3 and 171.7‰ for HNO₃, HCl and LiCl respectively.

^e $\delta^{57}\text{Fe}/^{56}\text{Fe}$ corrected for errors in recovery and for partial re-equilibration during the separation of ferrous and ferric phases.

^f F values calculated based on corrected $\delta^{57/56}\text{Fe}$.

^g Values corrected for partial re-equilibration using uncorrected rate coefficients.

* Data corrected for errors in recovery using equation 8.

species was +330.9 ‰, and the $\delta^{57/56}\text{Fe}$ of the Fe(II) species was -1.0 ‰. Solutions of ferrous and ferric iron were mixed and allowed to react over a period of seconds to minutes before separation of Fe(III) from Fe(II) by addition of BaCO₃. Results of the kinetic experiments run in 0, 11, and 110 mM Cl⁻ solutions at 22°C and 0°C are listed in Table 3 and plotted in Figure 2. In the initial stages of all experiments, the measured $\delta^{57/56}\text{Fe}$ of the ferric phase decreases rapidly with time, with a corresponding increase in the $\delta^{57/56}\text{Fe}$ of the ferrous phase as isotopic exchange occurs. At 22°C, the ferric and ferrous components have moved ~60–90% towards isotopic equilibrium within the first 5 seconds, and the system closely reaches equilibrium within 60 seconds ($F > 0.95$); attainment of isotopic equilibrium is shown by no further changes in the $\delta^{57/56}\text{Fe}$ values for ferrous and ferric components (see Table 3, Fig. 2). As expected, the approach to equilibrium in the 0°C experiments is substantially slower. There is considerable variability in the measured values of $\delta^{57/56}\text{Fe}$ for both ferric and ferrous fractions in the early time points primarily due to incomplete separation of the ferrous and ferric components, in addition to possible continued exchange during filtration and separation of the mixtures. It is important to note that these effects are more conspicuous in the isotopically enriched experiments, as opposed to experiments that use “isotopically normal” solutions because the isotopic contrasts in the kinetic experiments are so large.

The extent of exchange towards isotopic equilibrium can be described by

$$F = \left(\frac{\delta - \delta_i}{\delta_e - \delta_i} \right) \quad (5)$$

where δ is the isotopic composition at any time, δ_i is the isotopic composition of the starting material, and δ_e is the equilibrium isotopic composition calculated from the relative masses and isotopic composition of the ferrous and ferric starting solutions (see Johnson et al., 2002a, and references therein). Calculation of F using either ferrous or ferric species should yield similar results (Table 3), assuming that separation is quantitative and rapid compared to the exchange rate, and

that the reaction between the ferrous and ferric Fe does not proceed via the oxidation and reduction of other species; this is an important assumption that gains support from the reported insensitivity of the exchange kinetics to the presence of oxygen (Eimer et al., 1952). If small amounts of either ferrous or ferric iron are trapped in the other phase, measured $\delta^{57/56}\text{Fe}$ values will be either too light or too heavy, with subsequent errors in the calculated F values. Although this is potentially a significant problem in experiments using the ⁵⁷Fe-enriched tracers, this is a lesser problem in the equilibrium experiments that have isotopically normal compositions (see discussion below). Overall, we feel that the kinetics of Fe isotope exchange are best constrained from the Fe(II) data, because incomplete recoveries are typically a result of oxidation of Fe(II), resulting in its incorporation into the Fe(III) fraction. Although such incomplete yields bias the Fe(III) fraction to low $\delta^{57/56}\text{Fe}$ values, this will not affect the $\delta^{57/56}\text{Fe}$ of the Fe(II) fraction.

Substituting F into a general rate equation produces

$$\frac{-d(1-F)}{dt} = K_n(1-F)^n \quad (6)$$

where K is the rate coefficient and n is the order of the reaction. The kinetics and mechanism of ferrous-ferric exchange have been discussed in the literature (e.g., Silverman and Dodson, 1952; Hudis and Dodson, 1956; Brunschwig et al., 1982; Haim, 1983; Sutin, 1983; 1999), but our sole purpose here is to apply a correction for the possible exchange taking place during separation. Previous experimental work in our laboratory (see Johnson et al., 2002a, and references therein) demonstrates that the ferrous-ferric isotopic exchange in solution can be well fit as a second order rate equation ($n = 2$), such that

$$\frac{F}{(1-F)} = K_2t \quad (7)$$

Fitting the exchange kinetics as a second order reaction allows us to assess the maximum error (see appendix) in the measured isotope values associated with partial exchange of the

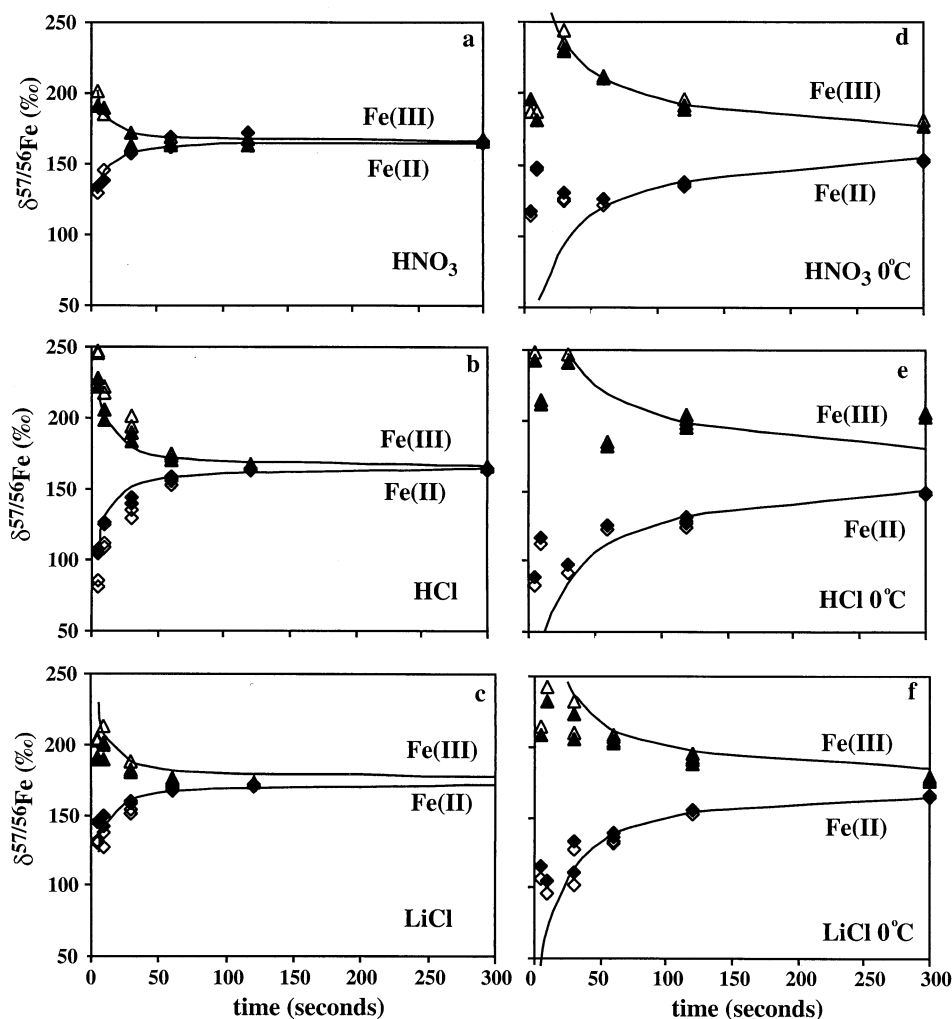


Fig. 2. Determination of ferrous-ferric exchange kinetics using ^{57}Fe -enriched tracer solutions. Measured $\delta^{57/56}\text{Fe}$ for ferrous (\blacklozenge)-ferric (\blacktriangle) exchange kinetic experiments versus time. Corrected $\delta^{57/56}\text{Fe}$ for ferrous (\diamond)-ferric (\triangle). Initial $\delta^{57/56}\text{Fe}$ are Fe(II) ~ 0 ‰ and Fe(III) ~ 331 ‰ (see text and Table 2). Ferrous and ferric components reach isotopic equilibrium within seconds to minutes after mixing. (a) Ferrous-ferric exchange in 10 mM HNO_3 (0 mM Cl^-) at 22°C, (b) 10 mM HCl at 22°C, (c) 10 mM HCl + 100 mM LiCl at 22°C, (d) 10 mM HNO_3 at 0°C, (e) 10 mM HCl at 0°C, (f) 10 mM HCl + 100 mM LiCl at 0°C. Lines are the best fit curve for either ferrous or ferric for the second order rate equation using the uncorrected rate coefficients.

ferrous and ferric species during separation (see discussion below). Our data cannot be easily fit as a zero order reaction, though the exchange kinetics could also be reasonably fit as a first-order reaction with respect to either ferrous or ferric Fe with good agreement between the rate coefficients determined in this study and previous work (see Appendix). Although it is possible to fit the data as a higher-order reaction, there are insufficient data to justify such an order.

The experimentally determined rate coefficient assuming second order exchange reaction for the six kinetic experiments can be calculated from a linear fit of $F/(1-F)$ versus time (Fig. 3, Table 4). Ferrous-ferric isotopic exchange rates are significantly faster in the HNO_3 and LiCl solutions than in the HCl solution. Exchange rates are about an order of magnitude faster at room temperature (22°C) than at 0°C.

3.3.2. Corrections to measured isotopic compositions

We can correct the measured isotopic compositions, calculated F , and resultant isotopic exchange rates for incomplete separation and recovery of ferrous and ferric components, and partial re-equilibration of ferrous and ferric species during precipitation.

3.3.2.1. Fe separation and recovery. With the exception of the exchange experiment using LiCl solution at 0°C, the K values calculated for the ferrous species are systematically lower than those calculated for the ferric species. This is consistent with an incomplete recovery of ferrous iron, as determined by *Ferrozine* measurements of total Fe, which results in higher F and higher K values for the ferric species (see Table 3). Because the isotopic fractionation associated with precipitation of ferrous

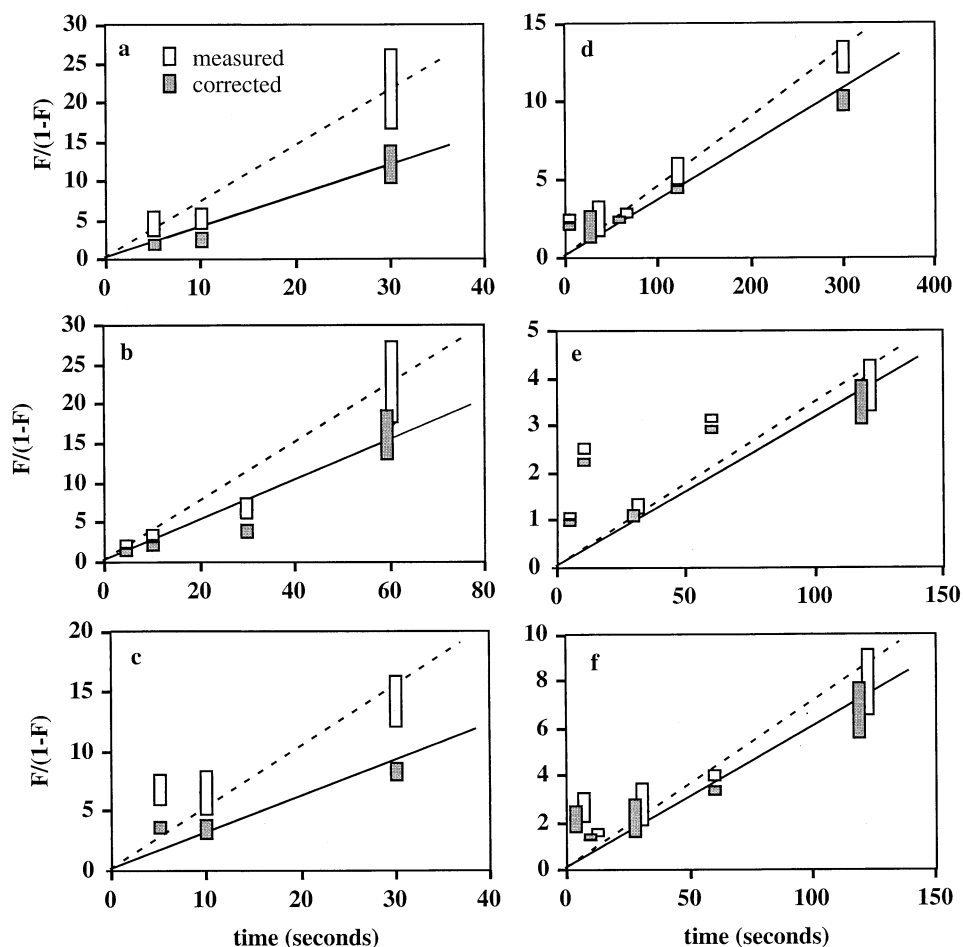


Fig. 3. Second-order rate relations for ^{57}Fe -enriched experiments cast as $F/(1-F)$ versus time for all six sets of kinetic experiments based on measured $\delta^{57/56}\text{Fe}$ values for ferrous and ferric phases (white bar). (a) Ferrous-ferric exchange in 10 mM HNO_3 (0 mM Cl^-) at 22°C, (b) 10 mM HCl at 22°C, (c) 10 mM HCl + 100 mM LiCl at 22°C, (d) 10 mM HNO_3 at 0°C, (e) 10 mM HCl at 0°C, (f) 10 mM HCl + 100 mM LiCl at 0°C. The slope of a linear fit of $F/(1-F)$ versus time with the intercept set at 0 (required for the second order kinetic equation) yields the rate coefficient K . The dashed line is the best fit through the uncorrected ferrous and ferric data. Gray bars and solid line are for $F/(1-F)$ values calculated from $\delta^{57/56}\text{Fe}$ that have been corrected for partial re-equilibration during precipitation and for incomplete separation of the ferrous and ferric phases during the precipitation experiments (see Table 3). Corrected data show a significantly improved fit in terms of 0 intercept and better agreement between F values calculated for ferrous and ferric components.

Fe in the ferric phase is not significant compared with the extreme isotopic enrichment involved in the kinetic experiments, we can estimate the $\delta^{57/56}\text{Fe}$ for the ferric phase from a simple mixing calculation where the measured $\delta^{57/56}\text{Fe}$ is equal to the relative contributions of ferrous and ferric iron and the $\delta^{57/56}\text{Fe}$ for ferrous iron that was sequestered in the ferric phase:

$$\delta_{\text{mix}} = \delta_{\text{Fe(III)}}X_{\text{Fe(III)}} + \delta_{\text{Fe(II)}}X_{\text{Fe(II)}} \quad (8)$$

Where $X_{\text{Fe(III)}}$ and $X_{\text{Fe(II)}}$ are determined by Ferrozine analysis. This correction is largest (up to $\sim 5\%$) for the extreme isotopic compositions that are associated with the earlier time points where the difference in the $\delta^{57/56}\text{Fe}$ between the ferrous and ferric phases is the largest. In some experiments we did not apply this correction because there was no significant systematic error in iron recovery (beyond the $\sim 5\%$ analytical error associated with the *Ferrozine* analysis).

For the 60 and 120 second time points in the 22°C HNO_3 experiment (see Fig. 2a and Table 3), the measured $\delta^{57/56}\text{Fe}$ in the ferrous fraction is ~ 2 to 4 ‰ heavier than that of the equilibrium value. We attribute this to slight cross contamination by the ferric solution in the dead volume of the syringe filter before equilibration with the bulk solution, producing a measured $\delta^{57/56}\text{Fe}$ for the recovered ferrous component that is too high. Because the analytical error in Fe recovery is greater than that associated with contamination in the dead volume, we have not corrected our measured $\delta^{57/56}\text{Fe}$ values for this problem. In other experiments, the ferrous solution was pipetted to the syringe first, eliminating this error.

3.3.2.2. Partial re-equilibration. Another source of uncertainty in the measured $\delta^{57/56}\text{Fe}$ values arises through the partial re-equilibration of ferrous-ferric Fe in solution during the pre-

Table 4. Measured and corrected rate constants K (s^{-1}) obtained from kinetics experiments. Rate constants calculated from a linear fit of $F/(1 - F)$ (Figure 3) for ferrous, ferric, and average of the two components.

	Uncorrected		Average	Corrected		Average
	Fe(II)	Fe(III)	Fe(II) + (III)	Fe(II)	Fe(III)	Fe(II) + (III)
HNO ₃ 22°C	0.64 ± 0.04	0.86 ± 0.07	0.71 ± 0.05	0.43 ± 0.03	0.36 ± 0.03	0.39 ± 0.03
HCl 22°C	0.34 ± 0.04	0.41 ± 0.03	0.38 ± 0.03	0.25 ± 0.03	0.27 ± 0.03	0.25 ± 0.02
LiCl 22°C	0.47 ± 0.05	0.55 ± 0.08	0.51 ± 0.05	0.29 ± 0.03	0.32 ± 0.04	0.30 ± 0.02
HNO ₃ 0°C	0.041 ± 0.005	0.046 ± 0.002	0.044 ± 0.003	0.037 ± 0.004	0.031 ± 0.002	0.035 ± 0.002
HCl 0°C	0.034 ± 0.007	0.034 ± 0.007	0.034 ± 0.005	0.031 ± 0.006	0.031 ± 0.007	0.031 ± 0.004
LiCl 0°C	0.076 ± 0.005	0.066 ± .007	0.071 ± 0.004	0.063 ± 0.004	0.055 ± 0.006	0.060 ± 0.004
22 mM HCl*			0.26 ± 0.06			0.18 ± 0.03

* Data from Johnson et al. (2002) for ~22 mM Cl⁻ at pH ~2.5 and 22°C.

precipitation reaction. Based on our observations of precipitate formation after addition of the BaCO₃ suspension, it appears that mixing and precipitation of the ferric oxyhydroxide phases goes to completion rapidly, <1 second at 22°C, and <2 seconds in the 0°C experiments. Using the rate constants based on ferrous and ferric data derived from the measured $\delta^{57/56}\text{Fe}$ values (Table 4), we estimate that 28 to 42% isotopic exchange may occur during precipitation and separation at 22°C, and 7 to 13% in the 0°C experiments (Table 5). Based on the estimates for extent of isotopic exchange during the separation, we can correct the measured $\delta^{57/56}\text{Fe}$ values for errors in partial re-equilibration during precipitation (Table 3).

There is generally much better agreement between the corrected F values as calculated from the ferrous and ferric fractions than for the uncorrected measurements, confirming that the corrected data better constrain the true rate coefficients (Table 4, Fig. 3). In addition, use of the corrected data provides an improved overall fit of the second-order rate equation. These revisions to the rates of exchange in turn provide revised estimates of the extent of partial re-equilibration during precipitation, and these are 21 to 28% exchange in 1 second at 22°C and 6 to 11% exchange in 2 seconds at 0°C (Table 5).

3.3.3. Equilibrium Fe fractionation

The aqueous equilibrium Fe(III)-Fe(II) fractionation was determined for mixed Fe solutions at pH ~2, at temperatures of

0 and 22°C, Cl⁻ concentration (0, 11, and 111 mM) and Fe(II)/Fe_{Total} ratios of ~0.2, 0.5, 0.8, as a test for isotopic mass balance. The speciation, pH, and Cl⁻ contents of the equilibrium experiments match those used in the companion ⁵⁷Fe-enriched kinetic experiments. Aliquots of ferrous and ferric solutions were mixed and allowed to equilibrate for hours to days before separation of the ferric phase by precipitation (Table 1); as noted above, the ferric/ferrous ratios of all solutions were stable over the time allowed for complete isotopic equilibration.

Although the initial ferrous and ferric solutions all have $\delta^{56}\text{Fe}$ of ~0 ‰, after mixing, the ferrous component is always isotopically light compared to the ferric component (Table 6, Fig. 4). The average uncorrected $\Delta_{\text{Fe(III)-Fe(II)}}$ fractionation determined for mixtures of ferrous and ferric iron in dilute acid solutions, 10 mM HNO₃, 10 mM HCl and 10 mM HCl + 100 mM LiCl at room temperature were nearly identical at +2.76 ± 0.09 ‰, +2.87 ± 0.22 ‰, and +2.76 ± 0.06 ‰ respectively (Table 6 and 7). This is very similar to the value measured by Johnson et al. (2002a), who estimated the measured $\Delta_{\text{Fe(III)-Fe(II)}}$ as 2.75 ± 0.15 ‰ for dilute chloride solutions. Partitioning of the heavy isotope into the ferric phase is expected, considering the shorter bond length of ~2.0 Å for Fe(III)-O (water) versus 2.1 Å for Fe(II)-O (water) (Brunschwig et al., 1982), and the lower vibrational frequencies for ferrous Fe (389 cm⁻¹ for [Fe^{II}(H₂O)₆]²⁺ and 505 cm⁻¹ for [Fe^{III}(H₂O)₆]³⁺ for ν_3 ;

Table 5. Predicted F values.

Seconds	22°C HNO ₃	22°C HCl	22°C LiCl	0°C HNO ₃	0°C HCl	0°C LiCl
	Predicted F values from the measured rate coefficient					
1	0.42	0.28	0.35	0.05	0.04	0.07
2	0.59	0.43	0.53	0.09	0.07	0.13
3	0.68	0.53	0.63	0.12	0.10	0.19
4	0.74	0.60	0.70	0.15	0.13	0.23
5	0.78	0.65	0.75	0.19	0.15	0.28
	Predicted F values from the corrected rate coefficient					
1	0.28	0.21	0.23	0.04	0.04	0.06
2	0.44	0.34	0.38	0.07	0.06	0.11
3	0.54	0.43	0.47	0.10	0.09	0.16
4	0.61	0.51	0.55	0.13	0.12	0.20
5	0.66	0.56	0.60	0.15	0.14	0.24

Predicted proportion of re-equilibration of Fe(II) and Fe(III) as a function of time during separation, as well as those corrected for partial re-equilibration (see Table 4). Values in bold reflect those estimated to be applicable to the separation times of the experiments.

Table 6. Data for equilibrium experiments.

Sample ^a	Fe(II)/ Fe _{total} ^b	Ferrous				Ferric				$\Delta_{\text{Fe(III)-Fe(II)}}$	
		$\delta^{56}\text{Fe}^c$	$\delta^{57}\text{Fe}^c$	$\mu\text{g Fe}^d$	% rec ^e	$\delta^{56}\text{Fe}^c$	$\delta^{57}\text{Fe}^c$	$\mu\text{g Fe}^d$	% rec ^e	meas ^f	cor ^g
HNO ₃ experiments at 22°C											
DB1	0.52	-0.88 ± 0.07	-1.33 ± 0.04	107	108	1.76 ± 0.06	2.70 ± 0.04	80.1	88.1	2.64 ± 0.06	3.00 ± 0.06*
DB3	0.52	-0.88 ± 0.09	-1.33 ± 0.05	103	104	1.57 ± 0.07	2.25 ± 0.04	103	113	2.71 ± 0.15	2.93 ± 0.15
		-1.24 ± 0.08	-1.74 ± 0.07			1.36 ± 0.05	2.07 ± 0.03				
DB4	0.21	-1.63 ± 0.06	-2.43 ± 0.04	40.9	104	1.43 ± 0.07	2.08 ± 0.04	150	103	2.27 ± 0.08	2.60 ± 0.08
		-1.24 ± 0.06	-1.82 ± 0.03			0.60 ± 0.11	0.98 ± 0.07				
DB6	0.21	-1.99 ± 0.01	-2.86 ± 0.02	45.6	116	0.68 ± 0.10	1.01 ± 0.05	137	94.0	2.86 ± 0.11	3.33 ± 0.11*
		-1.63 ± 0.06	-2.43 ± 0.04			0.95 ± 0.10	1.29 ± 0.05				
DB9	0.81	-0.46 ± 0.06	-0.61 ± 0.04	158	100	2.29 ± 0.07	3.40 ± 0.05	50.2	138	2.75 ± 0.09	2.92 ± 0.09
DH2	0.51	-1.13 ± 0.08	-1.63 ± 0.04	98.3	97.5	1.63 ± 0.06	2.36 ± 0.03	92.4	101	2.74 ± 0.06	2.96 ± 0.06
		-1.10 ± 0.07	-1.61 ± 0.07								
DH3	0.51	-1.26 ± 0.06	-1.78 ± 0.04	96.4	95.6	1.58 ± 0.06	2.36 ± 0.04	91.2	99.2	2.83 ± 0.08	3.05 ± 0.08
DH4	0.21	-1.57 ± 0.07	-2.30 ± 0.03	43.0	107	0.67 ± 0.06	1.07 ± 0.03	138	93.7	2.30 ± 0.10	2.67 ± 0.10*
		-1.68 ± 0.08	-2.41 ± 0.04								
Starting solutions for DB and DH experiments ^h											
		0.36 ± 0.06	0.54 ± 0.03			0.28 ± 0.05	0.41 ± 0.03				
		0.15 ± 0.10	0.20 ± 0.04			0.28 ± 0.05	0.41 ± 0.03				
Mixtures of starting solutions ⁱ											
5FeII + 5FeIII		0.11 ± 0.08	0.17 ± 0.05								
8FeIII + 2FeII		0.15 ± 0.09	0.29 ± 0.05								
2FeII + 8FeIII		0.19 ± 0.12	0.24 ± 0.05								
GB1	0.51	-1.14 ± 0.06	2.68 ± 0.08	96.2	99.5	1.54 ± 0.06	2.27 ± 0.04	99.6	107	2.68 ± 0.08	2.90 ± 0.08
GB2	0.51	-1.29 ± 0.08	2.89 ± 0.12	97.9	101	1.59 ± 0.09	2.31 ± 0.05	99.4	107	2.89 ± 0.12	3.11 ± 0.12
Starting solutions for GB experiments ^h											
		0.20 ± 0.07	0.23 ± 0.04			0.13 ± 0.07	0.21 ± 0.04				
Mixtures of starting solutions ⁱ											
5FeII + 5FeIII		0.19 ± 0.05	0.32 ± 0.03								
8FeIII + 2FeII		0.24 ± 0.06	0.27 ± 0.03								
2FeII + 8FeIII		0.20 ± 0.05	0.26 ± 0.04								
HCl experiments at 22°C											
DF1	0.49	-1.34 ± 0.06	-1.93 ± 0.03	82.0	85.0	1.47 ± 0.08	2.09 ± 0.05	98.8	98.5	2.83 ± 0.08	3.00 ± 0.08
DF5	0.19	-1.38 ± 0.13	-1.99 ± 0.05	33.6	87.0	0.69 ± 0.7	0.95 ± 0.03	156	97.1	2.82 ± 0.14	3.06 ± 0.14
		-2.04 ± 0.04	-3.02 ± 0.03			0.87 ± 0.13	1.07 ± 0.06				
DF6	0.19	-2.10 ± 0.07	-3.04 ± 0.05	36.5	94.6	0.73 ± 0.04	1.07 ± 0.03	156	97.1	2.83 ± 0.08	3.07 ± 0.08
DF9	0.79	-0.44 ± 0.13	-0.76 ± 0.06	140	90.6	2.03 ± 0.07	3.03 ± 0.04	49.6	124	2.57 ± 0.16	2.72 ± 0.16*
DG3	0.49	-1.35 ± 0.04	-1.95 ± 0.03	101	102	1.50 ± 0.04	2.23 ± 0.04	99.0	98.4	2.85 ± 0.06	3.02 ± 0.06
DG4	0.20	-1.75 ± 0.05	-2.68 ± 0.03	44.9	114	0.69 ± 0.06	1.00 ± 0.03	153	95.1	2.44 ± 0.08	2.78 ± 0.08*
DG8	0.80	-0.61 ± 0.06	-0.84 ± 0.03	153	96.8	2.49 ± 0.03	3.87 ± 0.01	42.2	105	3.10 ± 0.07	3.24 ± 0.07
D12	0.49	-1.48 ± 0.15	-2.15 ± 0.06	101	96.6	1.53 ± 0.04	2.22 ± 0.03	103	102	2.91 ± 0.07	3.08 ± 0.07
D14	0.20	-1.85 ± 0.05	-2.71 ± 0.03	44.9	104	0.52 ± 0.04	0.84 ± 0.02	164	102	2.38 ± 0.06	2.62 ± 0.06
D19	0.80	-0.63 ± 0.05	-0.90 ± 0.03	153	100	2.43 ± 0.04	3.65 ± 0.03	41.1	102	3.06 ± 0.06	3.20 ± 0.06
Starting solutions for HCl experiments ^h											
FeCl ₂		0.03 ± 0.07	0.16 ± 0.04			0.00 ± 0.07	0.03 ± 0.04				
LiCl experiments at 22°C											
HC2	0.50	-1.48 ± 0.08	-2.15 ± 0.05	99.3	104	1.35 ± 0.04	1.92 ± 0.03	101	104	2.83 ± 0.09	3.01 ± 0.09
HC6	0.20	-1.72 ± 0.07	-2.65 ± 0.04	40.9	101	0.65 ± 0.07	0.83 ± 0.05	156	101	2.36 ± 0.10	2.63 ± 0.10
HC8	0.80	-0.54 ± 0.08	-0.99 ± 0.09	155	97.5	2.17 ± 0.05	2.86 ± 0.03	37.7	97.5	2.71 ± 0.10	2.86 ± 0.10
HC9	0.80	-0.89 ± 0.07	-1.25 ± 0.05	158	102	1.86 ± 0.06	2.76 ± 0.04	39.3	102	2.75 ± 0.09	2.90 ± 0.09
Starting solutions for LiCl experiments ^h											
Fe(II)Cl ₂		-0.37 ± 0.07	-0.56 ± 0.03			0.09 ± 0.05	0.17 ± 0.03				
Mixtures of starting solutions ⁱ											
5FeII + 5FeIII		-0.11 ± 0.04	-0.18 ± 0.04								
8FeIII + 2FeII		0.00 ± 0.06	0.04 ± 0.04								
2FeII + 8FeIII		-0.24 ± 0.05	-0.46 ± 0.03								
HNO ₃ experiments at 0°C											
ja1	0.52	-1.49 ± 0.06	-2.14 ± 0.03	107	107	1.94 ± 0.05	2.87 ± 0.03	102	109	3.43 ± 0.08	3.52 ± 0.08
ja3	0.52	-1.74 ± 0.06	-2.57 ± 0.03	95.5	95.8	2.03 ± 0.05	3.00 ± 0.03	95.4	102	3.77 ± 0.08	3.86 ± 0.08
jd3	0.52	-1.20 ± 0.05	-1.69 ± 0.03	112	112	1.77 ± 0.05	2.63 ± 0.02	86.6	92.7	2.97 ± 0.07	3.28 ± 0.07*
jd4	0.21	-2.12 ± 0.05	-3.17 ± 0.03	46.3	116	0.95 ± 0.05	1.37 ± 0.03	145	97.3	3.07 ± 0.07	3.19 ± 0.07
jd8	0.81	-0.61 ± 0.08	-0.85 ± 0.03	149	93.5	2.21 ± 0.06	3.29 ± 0.03	50.6	135	2.82 ± 0.09	3.12 ± 0.09*
jd9	0.81	-0.78 ± 0.05	-1.11 ± 0.03	148	93.0	2.51 ± 0.07	3.90 ± 0.33	57.7	154	3.25 ± 0.09	3.74 ± 0.09*
		-0.70 ± 0.09	-1.01 ± 0.05								

Table 6. (Continued)

Sample ^a	Fe(II)/ Fe _{total} ^b	Ferrous				Ferric				$\Delta_{\text{Fe(III)-Fe(II)}}$	
		$\delta^{56}\text{Fe}^c$	$\delta^{57}\text{Fe}^c$	$\mu\text{g Fe}^d$	% rec ^e	$\delta^{56}\text{Fe}^c$	$\delta^{57}\text{Fe}^c$	$\mu\text{g Fe}^d$	% rec ^e	meas ^f	cor ^g
Starting solutions for HNO ₃ experiments ^h											
		0.20 ± 0.07	0.23 ± 0.04			0.13 ± 0.07	0.21 ± 0.04				
Mixtures of starting solutions ⁱ											
5FeII + 5FeIII		0.19 ± 0.05	0.32 ± 0.03								
8FeIII + 2FeII		0.24 ± 0.06	0.27 ± 0.03								
2FeII + 8FeIII		0.20 ± 0.05	0.26 ± 0.04								
HCl experiments at 0°C											
jb1	0.48	-2.02 ± 0.06	-3.02 ± 0.03	94.9	102	1.64 ± 0.06	2.47 ± 0.03	92.4	96.8	3.66 ± 0.09	3.75 ± 0.09
jb5	0.19	-2.65 ± 0.05	-3.91 ± 0.03	40.5	109	0.71 ± 0.07	1.06 ± 0.04	151	98.9	3.36 ± 0.08	3.48 ± 0.08
jb9	0.79	-1.13 ± 0.04	-1.69 ± 0.03	152	102	2.36 ± 0.06	3.54 ± 0.03	39.7	104	3.47 ± 0.07	3.55 ± 0.07
		-1.07 ± 0.09	-1.43 ± 0.05								
fa9	0.80	-1.02 ± 0.05	-1.44 ± 0.04	144	96.1	2.32 ± 0.07	3.48 ± 0.04	39.3	106	3.34 ± 0.08	3.42 ± 0.08
Starting solutions for HCl experiments ^h											
		-0.37 ± 0.07	-0.56 ± 0.03			0.09 ± 0.05	0.17 ± 0.03				
Mixtures of starting solutions ⁱ											
5FeII + 5FeIII		-0.11 ± 0.04	-0.18 ± 0.04								
8FeIII + 2FeII		0.00 ± 0.06	0.04 ± 0.04								
2FeII + 8FeIII		-0.24 ± 0.05	-0.46 ± 0.03								
LiCl experiments at 0°C											
JC2	0.48	-2.10 ± 0.05	-3.08 ± 0.02	96.0	104	1.73 ± 0.06	2.46 ± 0.03	98.7	104	3.75 ± 0.07	3.84 ± 0.07
		-2.09 ± 0.05	-3.11 ± 0.03			1.62 ± 0.05	2.41 ± 0.03				
						1.62 ± 0.09	2.32 ± 0.05				
JC3	0.48	-1.97 ± 0.04	-2.87 ± 0.03	94.9	102	1.64 ± 0.07	2.45 ± 0.04	97.8	103	3.61 ± 0.08	3.70 ± 0.08
JC6	0.19	-2.42 ± 0.06	-3.52 ± 0.03	40.2	108	0.67 ± 0.05	1.07 ± 0.03	153	100	3.10 ± 0.05	3.22 ± 0.05
		-2.43 ± 0.12	-3.56 ± 0.05								
JC7	0.79	-1.01 ± 0.06	-1.49 ± 0.04	156	105	2.39 ± 0.06	3.51 ± 0.04	41.6	109	3.42 ± 0.03	3.54 ± 0.03
		-1.05 ± 0.05	-1.55 ± 0.03			2.39 ± 0.05	3.54 ± 0.03				
JC9	0.79	-1.02 ± 0.07	-1.48 ± 0.04	159	107	2.42 ± 0.07	3.57 ± 0.04	40.1	105	3.44 ± 0.09	3.52 ± 0.09
Starting solutions for LiCl experiments											
		-0.37 ± 0.07	-0.56 ± 0.03			0.09 ± 0.05	0.17 ± 0.03				

^a sample name

^b Fe(II)/Fe_{total} ratio based on ferrozine analysis of the starting solutions.

^c measured $\delta^{56}\text{Fe}$ and $\delta^{57}\text{Fe}$ for Fe recovered in the ferrous and ferric fractions. Errors are 2 standard errors from counting statistics

^d $\mu\text{g Fe}$ recovered in the ferrous and ferric fractions

^e percent recovery

^f measured $\Delta_{\text{Fe(III)-Fe(II)}} = \delta^{56}\text{Fe(III)} - \delta^{56}\text{Fe(II)}$

^g $\Delta_{\text{Fe(III)-Fe(II)}}$ corrected for errors due to partial re-equilibration

^h measured $\delta^{56}\text{Fe}$ and $\delta^{57}\text{Fe}$ for starting solutions

ⁱ measured $\delta^{56}\text{Fe}$ and $\delta^{57}\text{Fe}$ for mixtures of starting solutions

* experiments corrected for errors in recovery. If error in Fe recovery (for either Fe(II) or Fe(III)) based on *Ferrozine* measurements was >105% with a corresponding systematically low recover of the other Fe component, the $\delta^{56}\text{Fe}$ value of the component with the high recovery was corrected using equation 8.

195 cm⁻¹ and 304 cm⁻¹ for ν_4 , respectively; from Schauble et al. (2001), and references therein.

At 0°C, the average measured uncorrected $\Delta_{\text{Fe(III)-Fe(II)}}$ fractionations are significantly larger than for the room temperature experiments, +3.25 ± 0.38 ‰, +3.51 ± 0.14 ‰ and +3.56 ± 0.16 ‰ in 0, 11, and 111 mM Cl⁻ solutions, respectively. This increase in fractionation with decreasing temperature is in agreement with the theory of isotopic fractionation. Moreover, these results indicate that equilibrium Fe isotope fractionation between aqueous ferrous and ferric iron is essentially independent of the extent of Fe-chloride complexation within the range encompassed by our experiments.

3.3.4. Corrections to equilibrium isotopic measurements

Although the average measured $\Delta_{\text{Fe(III)-Fe(II)}}$ fractionations are nearly identical for experiments at a given temperature,

there is some variability within the data. As in the kinetic experiments, the measured isotope compositions should be corrected for incomplete separation of the ferrous and ferric components and partial re-equilibration during separation. A further potential source of error in the equilibrium experiments (but does not significantly affect the ⁵⁷Fe-tracer experiments) is kinetic and equilibrium isotope fractionation of Fe during precipitation of the ferric component as ferric oxyhydroxides.

3.3.4.1. Separation and recovery of Fe. A low Fe(II) yield results in a ferric fraction that is too low in its $\delta^{56}\text{Fe}$ value. Conversely, incomplete precipitation and flocculation of the ferric oxyhydroxides will make the ferrous phase heavy. Therefore, incomplete separation of Fe(II) and Fe(III) components results in a minimum $\Delta_{\text{Fe(III)-Fe(II)}}$ fractionation. This effect is generally more pronounced in experiments that have either

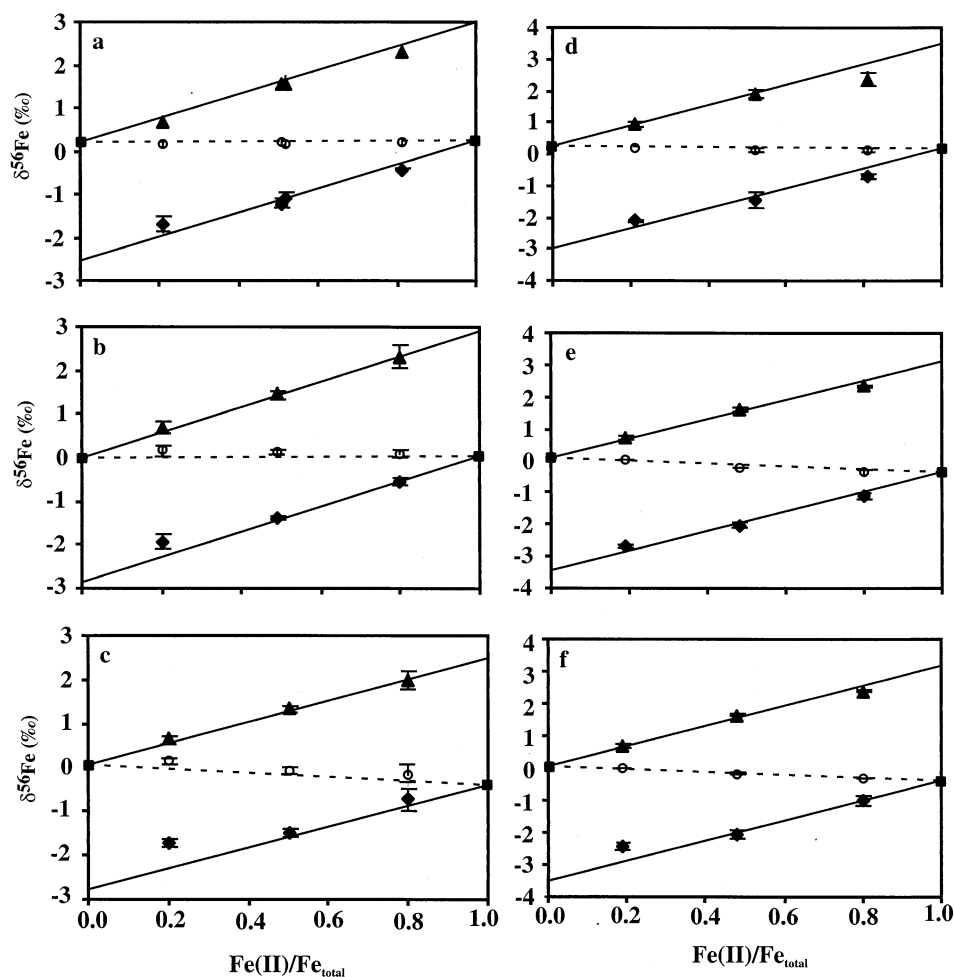


Fig. 4. Measured $\delta^{56}\text{Fe}$ values for ferrous(\blacklozenge) and ferric(\blacktriangle) components for the equilibrium experiments using Fe solutions with normal isotopic composition versus $\text{Fe(II)/Fe}_{\text{total}}$. Although initial isotopic compositions for the ferrous and ferric in the starting solutions are ~ 0 ‰ (see Table 6), after mixing, the lighter isotopes are partitioned into the ferrous species, while the heavier isotopes are concentrated in the ferric species. (\circ) represents calculated isotopic mass-balance based on measured $\delta^{56}\text{Fe}$ and Fe recovery for each ferrous-ferric pair. (a) Ferrous-ferric exchange in 10 mM HNO_3 (0 mM Cl^-) at 22°C, (b) 10 mM HCl at 22°C, (c) 10 mM HCl + 100 mM LiCl at 22°C, (d) 10 mM HNO_3 at 0°C, (e) 10 mM HCl at 0°C, (f) 10 mM HCl + 100 mM LiCl at 0°C. The average measured $\Delta_{\text{Fe(III)-Fe(II)}}$ in the three solutions are identical within experimental error at a constant temperature. Note deviation from the theoretical mass balance lines are most prominent for experiments with low $\text{Fe(II)/Fe}_{\text{total}}$ ratios, as predicted due to partial-re-equilibration during separation (Figs. 5 and 6)

high or low $\text{Fe(II)/Fe}_{\text{total}}$ ratios, or in the lower temperature experiments, where recovery was poorer due to slower flocculation. If the apparent recovery of either ferrous or ferric components after separation is $>100\%$, then we can estimate the ‘true’ isotopic composition from simple mass balance calculations using a mixing equation (Eqn. 8) and the ferrous and ferric quantities determined by *Ferrozine* analysis. Corrections were applied for experiments where recovery of either the ferrous or ferric fraction was greater than 105%, with a corresponding systematic low recovery in the other Fe fraction.

3.3.4.2. Kinetic fractionation during precipitation. Previous experiments in our laboratory (e.g., Johnson et al., 2002a; Skulan et al., 2002) have demonstrated that extremely rapid precipitation (\sim seconds) produces no significant isotopic fractionation between Fe(II) in solution and the ferric-oxyhydrox-

ide precipitates (~ 0.2 ‰ uncertainty). Such an assessment assumes that there is no isotopic exchange between Fe(II) and colloidal Fe(III) oxyhydroxide. However, moderately rapid precipitation (hours) produced a precipitate that was ~ 1.3 ‰ lighter in $^{56}\text{Fe}/^{54}\text{Fe}$ ratios than Fe(III) in solution (Skulan et al., 2002). Such isotopic fractionations during ferric oxyhydroxide precipitation are a potential source of error in determining the true $\Delta_{\text{Fe(III)-Fe(II)}}$ fractionation of the aqueous ferric and ferrous components, although its effects can easily be calculated (Johnson et al., 2002a).

3.3.4.3. Partial re-equilibration. Another source of uncertainty in the measured $\Delta_{\text{Fe(III)-Fe(II)}}$ fractionation is the partial re-equilibration of dissolved ferrous and ferric phases during precipitation and separation. Corrections for partial re-equilibration in the equilibrium experiments are a function of the

Table 7. Average measured $\Delta_{\text{Fe(III)-Fe(II)}}$ and $\Delta_{\text{Fe(III)-Fe(II)}}$ corrected for partial re-equilibration and incomplete recovery. Average values exclude values for $\text{Fe(II)/Fe}_{\text{total}} = 0.2$ since these experiments were subject to larger errors in $\Delta_{\text{Fe(III)-Fe(II)}}$ (see discussion and Figure 5 and 6).

	$\Delta_{\text{Fe(III)-Fe(II)}}$	$\Delta_{\text{Fe(III)-Fe(II)}}$ corrected
HNO ₃ 22°C	2.76 ± 0.09	3.02 ± 0.14
HCl 22°C	2.87 ± 0.22	3.05 ± 0.17
LiCl 22°C	2.76 ± 0.06	2.92 ± 0.08
Average 22°C	2.80 ± 0.25	3.00 ± 0.23
HNO ₃ 0°C	3.25 ± 0.38	3.50 ± 0.31
HCl 0°C	3.51 ± 0.14	3.57 ± 0.17
LiCl 0°C	3.56 ± 0.16	3.65 ± 0.15
Average 0°C	3.44 ± 0.45	3.57 ± 0.38

Yorkfit to all data, assuming error in temperature of ±0.5 °C, produces the following regression:

$$10^3 \ln \alpha_{\text{Fe(III)-Fe(II)}} = \frac{[0.334 \pm 0.032] * 10^6}{T^2} - 0.88 \pm 0.38$$

For the Fe isotope fractionation between Fe(III) and Fe(II) as a function of temperature, T is in °K. Errors are 1 σ . Note this equation is only applicable over the range of Cl⁻ contents and Fe speciation encompassed by the current experiments.

Fe(II)/Fe_{total} ratio and these mass balance variations provide important checks on the accuracy of these corrections (Figs. 5 and 6). If we assume separation and precipitation at 22°C occurs within 1 s in the equilibrium experiments, the percent re-equilibration in the HNO₃, HCl, and LiCl experiments are 28, 21, and 23%, respectively (Table 5). Assuming an arbitrary $\Delta_{\text{Fe(III)-Ferric-oxide}}$ fractionation of ~+0.5 ‰, then the measured $\Delta_{\text{Fe(III)-Fe(II)}}$ fractionation would be 0.33 to 0.17, 0.24 to 0.14, and 0.27 to 0.15 ‰ too low (Table 6) for the HNO₃, HCl, and LiCl experiments (Fig. 5a), respectively. If precipitation were associated with a larger $\Delta_{\text{Fe(III)-Ferric-oxide}}$, perhaps ~+1 ‰, then the measured $\Delta_{\text{Fe(III)-Fe(II)}}$ would be ~0.2 to 0.5 ‰ too low (Fig. 5b). We note however, that we anticipate $\Delta_{\text{Fe(III)-Ferric-oxide}}$ to be near zero during very rapid precipitation (Skulan et al., 2002). The relatively large correction for experiments that have low Fe(II)/Fe_{total} ratios is consistent with the generally lower measured $\Delta_{\text{Fe(III)-Fe(II)}}$ for these experiments, and confirms the accuracy of these corrections (Figs. 5 and 6). Because the exchange kinetics are about an order of magnitude slower at 0°C, the corrections in $\Delta_{\text{Fe(III)-Fe(II)}}$ for partial re-equilibration will be ~0.1 ‰ or less.

Finally it is possible that the rapid change in pH that occurs during rapid precipitation of ferric oxyhydroxide may change the mechanism of isotopic exchange, particularly if this involved increased exchange rates through the hydroxyl pathway due to the transient increase in the $[\text{Fe}^{\text{III}}(\text{H}_2\text{O})_5(\text{OH})]^{2+}$ species. Although we cannot determine if such transient kinetic exchange is important in our experiments, such an effect would be accounted for in the corrections based on the ⁵⁷Fe-enriched kinetic experiments because these experiments were conducted in identical solutions and identical conditions as the equilibrium experiments.

3.4. Reduced Partition Function Ratios

Schauble et al. (2001) calculated the reduced partition function ratios (or β factors) for various Fe species using spectro-

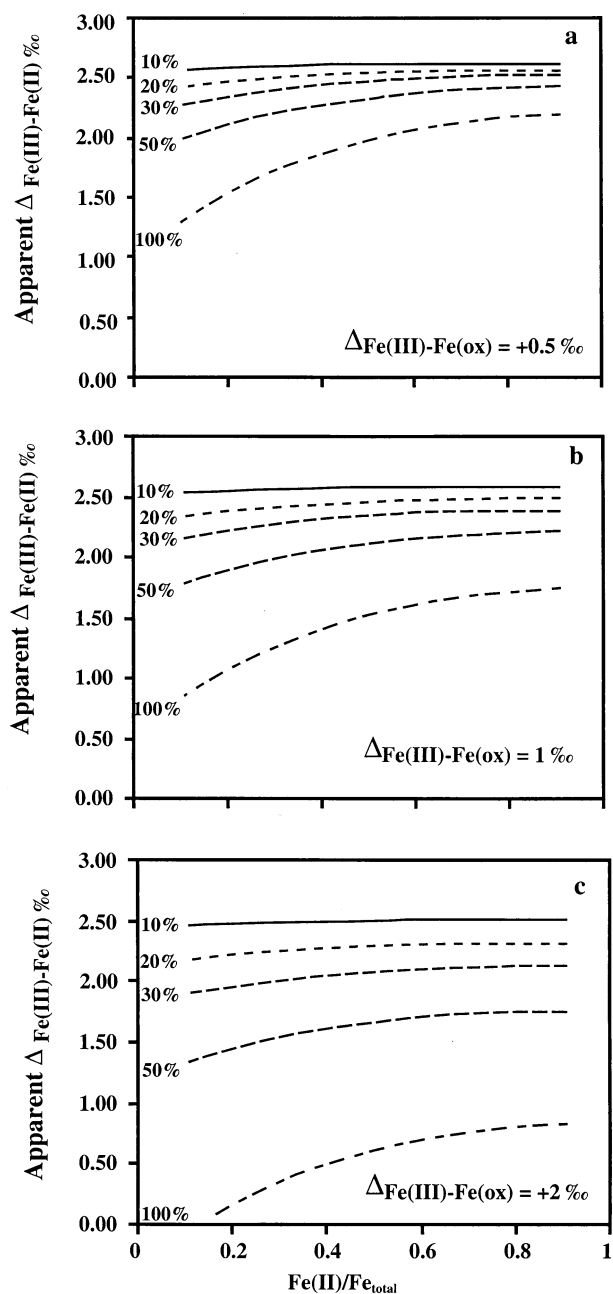


Fig. 5. Apparent $\Delta_{\text{Fe(III)-Fe(II)}}$ as a function of $\text{Fe(II)/Fe}_{\text{total}}$ for 10, 20, 30, 50 and 100% partial re-equilibration for (a) $\Delta_{\text{Fe(III)-Fe(oxide)}} = +0.5 \text{ ‰}$, (b) $\Delta_{\text{Fe(III)-Fe(oxide)}} = +1 \text{ ‰}$, (c) $\Delta_{\text{Fe(III)-Fe(oxide)}} = +2 \text{ ‰}$. Based on exchange kinetics determined from the ⁵⁷Fe tracer experiments, the extent of partial re-equilibration that could occur during precipitation and separation is estimated to be ~21 to 28% at 22°C and ~10% at 0°C. Note that the largest errors introduced due to partial re-equilibration are for the experiments that have low $\text{Fe(II)/Fe}_{\text{total}}$ ratios, consistent with the observed data (Fig. 4)

scopic data. The $\Delta_{\text{Fe(III)-Fe(II)}}$ fractionations that would be predicted for our experiments may be estimated by calculating the fractional contribution for specific Fe species. We assume that no fractionation occurs between $[\text{Fe}^{\text{III}}(\text{H}_2\text{O})_6]^{3+}$ and the deprotonated ferric complex $[\text{Fe}^{\text{III}}(\text{H}_2\text{O})_5(\text{OH})]^{2+}$ because of the

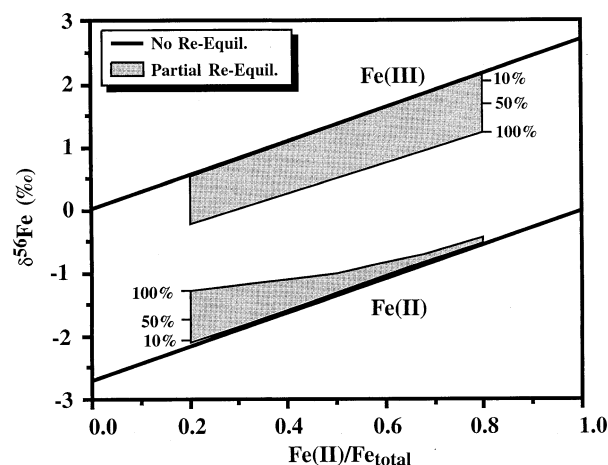


Fig. 6. Deviations in isotopic mass-balance constraints as a function of $\text{Fe(II)/Fe}_{\text{total}}$ due to the effects of partial isotopic re-equilibration, assuming $\Delta_{\text{Fe(III)-Fe(oxide)}} = +1$ ‰. Errors in estimating the true $\Delta_{\text{Fe(III)-Fe(II)}}$ are largest at lower $\text{Fe(II)/Fe}_{\text{total}}$ ratios, consistent with the observed data (Fig. 4).

very similar bonding environments of these species, and that the contribution of ferrous complexes other than $[\text{Fe}^{\text{II}}(\text{H}_2\text{O})_6]^{2+}$ is negligible. The predicted $\Delta_{\text{Fe(III)-Fe(II)}}$ for mixed ferric-ferrous solutions can then be calculated by

$$\Delta_{\text{Fe(III)-Fe(II)mix}} = \sum X_A \Delta_{\text{Fe(III-A)-Fe(II)}} \quad (9)$$

where X_A is the fraction of specific ferric species (e.g., $[\text{Fe}^{\text{III}}(\text{H}_2\text{O})_5\text{Cl}]^{2+}$), and $\Delta_{\text{Fe(III-A)-Fe(II)}}$ is the predicted equilibrium fractionation between this species and ferrous iron (e.g., $[\text{Fe}^{\text{III}}(\text{H}_2\text{O})_5\text{Cl}]^{2+}$ - $[\text{Fe}^{\text{II}}(\text{H}_2\text{O})_6]^{2+}$). Using this approach, the β factors presented by Schauble et al. (2001) suggest that the $\Delta_{\text{Fe(III)-Fe(II)}}$ fractionations should be +4.6 to 5.5 ‰ at 22°C,

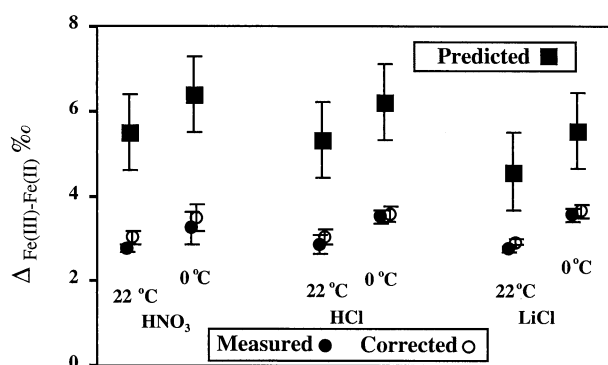


Fig. 7. Average measured $\Delta_{\text{Fe(III)-Fe(II)}}$ (●) and corrected $\Delta_{\text{Fe(III)-Fe(II)}}$ (○) for experiments at 0°C and 22°C in HNO_3 , HCl , and LiCl . The predicted $\Delta_{\text{Fe(III)-Fe(II)}}$ (■) calculated from reduced partition function ratios for Fe(III)-Fe(II) pairs from Schauble et al. (2001). In relating the predicted $\Delta_{\text{Fe(III)-Fe(II)}}$ for solutions containing a mixture ferric complexes, we assume the net fractionation is equal to the sum of the fraction of the Fe(III)-complex times the $\Delta_{\text{Fe(III)-Fe(II)}}$ for that complex. Schauble et al. (2001) estimate errors in the β factors to be $\sim +1$ ‰, which produces a net error in $\Delta_{\text{Fe(III)-Fe(II)}}$ of ~ 1.4 ‰. The measured $\Delta_{\text{Fe(III)-Fe(II)}}$ are only about half of the predicted values and the predicted shifts due to Cl^- substitution are not observed.

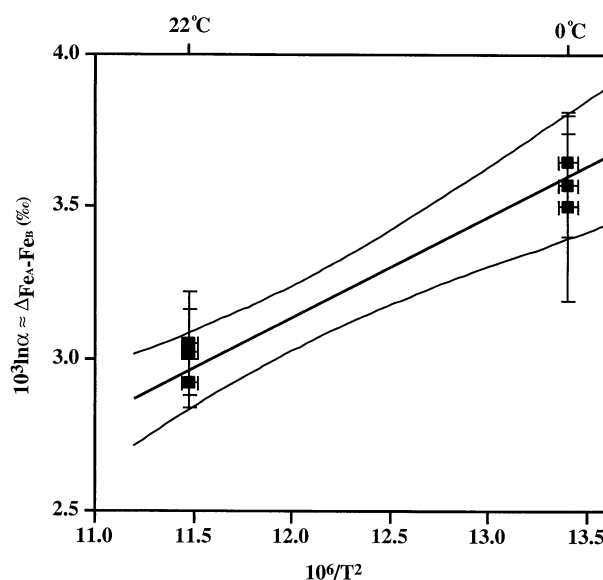


Fig. 8. The temperature dependence of $\Delta_{\text{Fe(III)-Fe(II)}}$ can be described as $\Delta_{\text{Fe(III)-Fe(II)}} = 10^3 \ln \alpha = A * 10^6 / T^2 + B$ where $A = 0.334 \pm 0.032$ and $B = -0.88 \pm 0.38$. T in °K. The $\Delta_{\text{Fe(III)-Fe(II)}}$ values are the average corrected values at 0°C and 22°C (see Table 8). The error in was taken as the square root of the sum of the squares for all of the $\Delta_{\text{Fe(III)-Fe(II)}}$ fractionation factors measured in this study for a particular temperature. The error in T was assumed to be ± 0.5 °C. Curved lines represent 1 σ confidence level for the slope.

and +5.3 to 6.4 ‰ at 0°C depending upon the $\text{Fe}^{\text{III}}\text{-Cl}^-$ speciation (Fig. 7), which is approximately half that measured in our experiments.

Because changes in octahedral chloride-bearing species over temperature ranges on the order of 100°C are relatively minor for the Cl^- contents encompassed by our experiments, we can use our data to calculate the temperature dependence of Fe(III)-Fe(II) fractionation in low-temperature environments through the relationship:

$$10^3 \ln \alpha_{\text{Fe(III)-Fe(II)}} = A * 10^6 / T^2 + B. \quad (10)$$

Where T is in °K. The coefficients A and B were calculated from a least-squares fit of the average $\Delta_{\text{Fe(III)-Fe(II)}}$ fractionation at 22 and 0°C using the corrected fractionations in Table 7. Such a regression produces $A = 0.334 \pm 0.032$ and $B = -0.88 \pm 0.38$ (Table 7, Fig. 8). As an example of the effect moderately high temperatures may have, extrapolation to 100°C produces an equilibrium $\Delta_{\text{Fe(III)-Fe(II)}}$ of $+1.5 \pm 0.6$ ‰ for Fe -bearing solutions that had Fe speciation that was similar to those of our experiments. It is not yet known if this relation will hold for high Cl^- systems where significant tetrahedral Fe-Cl complexes may exist, which are predicted to have significantly different β factors than octahedral Fe complexes (Schauble et al., 2001).

4. DISCUSSION

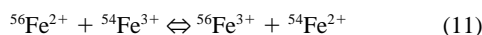
The reaction between ferrous and ferric iron can be described as a simple homogenous exchange reaction (Libby, 1952; Sutin, 1983; 1999; Haim, 1983; Duncan and Cook, 1968), with a

Table 8. Rate constants for ferrous-ferric exchange for different ferric species.

Exchanging species (omitting water of hydration)	rate* k (M ⁻¹ sec ⁻¹)
Fe(III) ³⁺ + Fe(II) ²⁺	1
Fe(III)OH ²⁺ + Fe(II) ²⁺	1000
Fe(III)L ²⁺ + Fe(II) ²⁺ (where L is Cl or F)	10

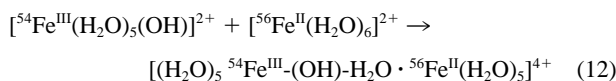
* Rate constants from Silverman and Dodson (1952) Hudis and Wahl (1953), and Sutin et al., (1961).

net exchange of one electron (t_{2g}) between two coexisting high-spin iron atoms that have different oxidation states. In terms of isotopic exchange, we can describe this reaction as:

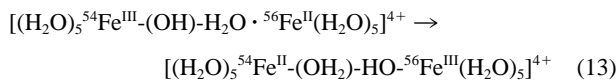


However, the direct exchange of electrons between two Fe atoms is unlikely to occur in aqueous solutions, because the cations are hydrated or complexed by other ligands. The exchange reaction can be described by three steps including the formation of an activated precursor complex, electron transfer (across a bridging hydroxyl, water, or chloride ion), and dissociation of the complex (Wehrli, 1990).

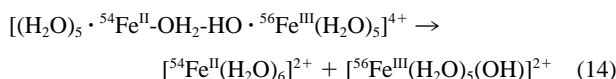
Precursor formation:



Electron transfer:



Dissociation of complex:



Similar equations can be written substituting the hexa-aquo ferric complex, or the ferric chloride complex for the ferric hydroxyl complex. The mechanism of the electron exchange reaction depends on the nature of the bridging ligand. Reactions between the ferric-hydroxyl and ferrous iron occur via an inner-sphere electron transfer; reactions between the two hexa-aquo species are thought to occur via an outer-sphere mechanism (e.g., Haim, 1983; Sutin, 1983; 1986; 1999; N. Sutin personal comm., 2002). Electron exchange reactions between ferrous- and ferric-chloride species can occur via an inner sphere electron transfer across a chloride bridge or via an outer sphere electron transfer involving either water or chloride (Haim, 1983; Sutin, 1999; Sutin et al., 1961; N. Sutin personal comm., 2002).

4.1. Kinetic Issues

The rate coefficient of $0.25 \pm 0.03 \text{ s}^{-1}$ that is calculated for the ferrous-ferric exchange reaction in dilute HCl at 22°C is slightly higher than that determined previously for similar conditions in our laboratory of $0.18 \pm 0.03 \text{ s}^{-1}$ (49 mM Cl⁻)

(Johnson et al., 2002a), and may reflect differences in Cl⁻ contents of the two experiments. The measured ferrous-ferric exchange rate coefficients are significantly larger for both the HNO₃ (0 mM Cl⁻) and LiCl experiments, at $0.39 \pm 0.03 \text{ s}^{-1}$ and $0.30 \pm 0.02 \text{ s}^{-1}$ respectively as compared to those of HCl-only systems. The exchange rates are about an order of magnitude slower at 0°C for all experiments. Although high concentrations of chloride in the LiCl experiments appears to catalyze the exchange reaction compared to the HCl experiments, we consistently measure faster ferrous-ferric exchange rates in the HNO₃ solutions, indicating that low levels of Fe(III)-Cl complexation appear to slightly inhibit the ferrous-ferric exchange reaction. It is well established, however, that chloride (and fluoride) catalyzes ferrous-ferric exchange (e.g., Silverman and Dodson, 1952; Hudis and Wahl, 1953; Sutin et al., 1961). Resolution of this apparent paradox lies in summing rates over all available pathways.

The kinetics of the exchange reaction in dilute acid solutions were investigated using radioactive ⁵⁵Fe over a range of pH, Fe and Cl⁻ concentration, and ionic strength (e.g., Silverman and Dodson, 1952; Hudis and Wahl, 1953; Hudis and Dodson 1956; Sutin et al., 1961). The rate of the reaction was determined to be first order with respect to Fe(II) and Fe(III), and can be described as:

$$R = [\text{FeII}][\text{FeIII}][k_w + k_H[\text{H}^+]^{-1} + k_L[\text{L}]^X] \quad (15)$$

where k_w is the rate constant for pH-independent exchange between Fe(II) and Fe(III), k_H is the pH-dependent rate constant for the exchange, and k_L is the rate constant for the ligand-promoted exchange. The reaction rate is strongly pH dependent, where k_H is ~1000 times larger than k_w , reflecting the increased reactivity of $[\text{Fe}^{\text{III}}(\text{H}_2\text{O})_5(\text{OH})]^{2+}$ as compared to $[\text{Fe}^{\text{III}}(\text{H}_2\text{O})_6]^{3+}$. Ferric complexation by Cl⁻ or F⁻ (e.g., $[\text{Fe}^{\text{III}}(\text{H}_2\text{O})_5\text{Cl}]^{2+}$) increases the exchange rate with ferrous iron by about a factor of 10 as compared to $[\text{Fe}^{\text{III}}(\text{H}_2\text{O})_6]^{3+}$ (Table 8).

Using the rate constants for the exchange reactions between ferrous and ferric species (Table 8), and the concentration of ferric and ferrous species calculated using PHREEQC (Table 2), we can estimate the contribution of each of the ferric species on the net reaction rate assuming:

$$R = k[\text{Fe(III)}][\text{Fe(II)}] \quad (16)$$

These calculations show that although Fe(III)-Cl complexation catalyzes the exchange reaction compared to hexa-aquo ferrous-ferric exchange by a factor of ~3 to 10, the effect is minimal compared to the net contribution of the $[\text{Fe}^{\text{III}}(\text{H}_2\text{O})_5(\text{OH})]^{2+}$ species (Table 9). Over 99% of the ferrous-ferric exchange occurs between $[\text{Fe}^{\text{II}}(\text{H}_2\text{O})_6]^{2+}$ and $[\text{Fe}^{\text{III}}(\text{H}_2\text{O})_5(\text{OH})]^{2+}$ in the HNO₃ and HCl solutions used in our experiments. Even in the LiCl experiment, where ~50% of the ferric ions are complexed by Cl⁻, the $[\text{Fe}^{\text{III}}(\text{H}_2\text{O})_5(\text{OH})]^{2+}$ species accounts for over 96% of the net ferrous-ferric exchange. Although Cl⁻ can function as a bridging ligand between ferrous and ferric ions, it is a weak σ donor, whereas OH⁻ is a better σ donor than either Cl⁻ or H₂O, and is also an excellent π donor to metals, and therefore can more readily facilitate electron exchange (Luther, 1990). Based on these calculations, we predict that the net measured ferrous-ferric

Table 9. Predictions of ferrous-ferric exchange rates at 22°C.

	Molal						Rates				
	Ferrous			Ferric			Fe(III)	Fe(III)OH	Fe(III)Cl	Total	R-Fe(OH)/T
	Fe ⁺²	Fe(OH) ⁺	FeCl ⁺	Fe ⁺³	Fe(OH) ⁺²	FeCl ⁺²					
HNO ₃	1.80E-04	5.32E-12		1.16E-04	6.21E-05		2.08E-08	1.12E-05		1.12E-05	0.998
HCl	1.78E-04	4.66E-12	1.78E-06	1.06E-04	5.06E-05	2.07E-05	1.90E-08	9.03E-06	3.70E-08	9.08E-06	0.994
LiCl	1.71E-04	3.02E-12	9.95E-06	6.58E-05	2.23E-05	7.84E-05	1.12E-08	3.80E-06	1.34E-07	3.95E-06	0.963

Concentrations of major ferrous and ferric species at 22°C calculated using PHREEQC and estimates of net exchange rate between $[\text{Fe}^{\text{II}}(\text{H}_2\text{O})_6]^{2+}$ and ferric species calculated assuming $R=K[\text{Fe}(\text{II})][\text{Fe}(\text{III})]$ ($\text{M} \cdot \text{s}^{-1}$). Rate constants K from Table 8. R-Fe(OH)/T is the rate calculated for Fe(II)-Fe(III) self exchange calculated for the ferric hydroxyl pathway divided by the sum of the exchange rates for all ferric species. The ferric-hydroxyl exchange pathway accounts for over 96% of the net reaction in our kinetic experiments.

exchange rates at a constant pH, ionic strength, temperature, and iron concentration should decrease with increasing Cl^- concentration, which is broadly consistent with our measured rates.

Because the rate of ligand substitution on either ferrous or ferric iron is rapid as compared to electron exchange, interactions between $\text{Fe}^{\text{III}}\text{X}^{2+}$ and $\text{Fe}(\text{II})^{2+}$ or $\text{Fe}(\text{III})^{3+}$ and $\text{Fe}^{\text{II}}\text{X}^+$ are kinetically equivalent (Taube, 1984). Assuming ligand substitution has a similar effect on ferrous reactivity with ferric species, we can estimate the net effect of different ferrous species on reaction rate. In the HCl solutions, $[\text{Fe}^{\text{II}}(\text{H}_2\text{O})_5\text{Cl}]^+$ comprises about 1% of the total ferrous species, but with its higher reactivity, this species might account for 10% of the net exchange rate. $[\text{Fe}^{\text{II}}(\text{H}_2\text{O})_5\text{OH}]^+$ represents only 3×10^{-8} of the total ferrous species. If the reactivity of $[\text{Fe}^{\text{II}}(\text{H}_2\text{O})_5\text{OH}]^+$ is ~ 1000 times greater than $[\text{Fe}^{\text{II}}(\text{H}_2\text{O})_6]^{2+}$, the $[\text{Fe}^{\text{II}}(\text{H}_2\text{O})_5\text{OH}]^+$ species should still have a negligible impact on the overall exchange reaction rate.

The relatively high exchange rate measured for the LiCl experiments may fundamentally reflect the overall high ionic strength of these solutions. Experimental studies on the kinetics of ferrous-ferric exchange have shown that electron exchange is facilitated at higher ionic strength solutions due to minimization of the electrostatic repulsion between ferrous and ferric iron (e.g., Brunschwig et al., 1980; 1982).

Although the kinetic pathways in which Fe isotope exchange occurs between aqueous ferric and ferrous species are important in considering the mechanisms of isotopic exchange, the kinetics of exchange can have no effect on the equilibrium isotope fractionation factors (Johnson et al., 2003b), contrary to what has been implied by Bullen et al. (2001; 2003). The very long time scales involved in our equilibrium experiments are more than sufficient to assure attainment of isotopic equilibrium, and any kinetic issues involved in the transient states of ferric oxyhydroxide precipitation are incorporated in the overall rates of exchange inferred from the ^{57}Fe -enriched kinetic experiments that were run under the same conditions as the equilibrium experiments.

4.2. Equilibrium Isotope Fractionation

The equilibrium $\Delta_{\text{Fe}(\text{III})-\text{Fe}(\text{II})}$ fractionations measured in this study at a constant temperature are identical within experimental error, $\sim +2.8$ ‰ at 22°C and $\sim +3.4$ ‰ at 0°C, regardless of the extent of Fe-Cl complexation (see Table 6 and 7).

Corrected for the effects of incomplete separation and partial re-equilibration during separation, we calculate the average true $\Delta_{\text{Fe}(\text{III})-\text{Fe}(\text{II})}$ fractionations to be $+3.0$ ‰ and $+3.6$ ‰ at 22°C and 0°C respectively (Table 7, Fig. 7). Although Johnson et al. (2002a) report a measured $\Delta_{\text{Fe}(\text{III})-\text{Fe}(\text{II})}$ of $+2.75$ ‰, this value was not corrected for uncertainties associated with species separation, and we recommend using the corrected values reported here, based on the more exhaustive experimental determination of the present study. Despite these small corrections, the measured $\Delta_{\text{Fe}(\text{III})-\text{Fe}(\text{II})}$ fractionation remains about half that predicted by Schauble et al. (2001). Moreover, we do not observe the effects of Cl^- substitution that are predicted by Schauble et al. (2001). For example, Schauble et al. (2001) predict a 1.5 ‰ difference in $\delta^{56}\text{Fe}$ values between $[\text{Fe}^{\text{III}}(\text{H}_2\text{O})_5\text{Cl}]^{2+}$ and $[\text{Fe}^{\text{III}}(\text{H}_2\text{O})_6]^{3+}$ at 22°C. Chloride substitution lowers the vibrational frequency of the Fe-Cl bond pair as compared to Fe-O (248 versus 505 cm^{-1} for ν_3 , and 184 versus 304 cm^{-1} for ν_4 , from Schauble et al. (2001), and references therein), but this is offset by the higher mass of Cl^- and the greater sensitivity of the vibrational frequency to the mass of Fe. Therefore, we might expect significant isotopic fractionation between $[\text{Fe}^{\text{III}}(\text{H}_2\text{O})_{6-n}(\text{OH})_n]^{3-n}$ and $[\text{Fe}^{\text{III}}(\text{H}_2\text{O})_5\text{Cl}]^{2+}$.

Although some of the discrepancy between the predicted and observed fractionations may lie in uncertainties in the predicted β factors, it is not clear if this can entirely reconcile the differences. Schauble et al. (2001) estimate that the error associated with their individual β factors is ~ 1 ‰ at room temperature, although they note that some of the estimates for the reduced partition ratios, especially for $[\text{Fe}^{\text{III}}(\text{H}_2\text{O})_6]^{3+}$ and the mixed Fe^{III} -chloro complexes are based on incomplete data with unknown accuracy. The information used to derive the β factors is based on salts, which may not adequately reflect the vibrational spectra of dissolved ions. However, they also note that there is reasonable agreement for solid phases in the β factors calculated from vibrational spectra and those of Polyakov (1997) and Polyakov and Mineev (2000), which were based on modeling ^{57}Fe Mössbauer spectra.

Based on our experimental data, we suggest that if there is a fractionation between coexisting ferric species such as $[\text{Fe}^{\text{III}}(\text{H}_2\text{O})_6]^{3+}$ and $[\text{Fe}^{\text{III}}(\text{H}_2\text{O})_5\text{Cl}]^{2+}$, then it must be on the order of a few tenths per mil. If for example, the uncertainty in our measured $\Delta_{\text{Fe}(\text{III})-\text{Fe}(\text{II})}$ fractionation is ~ 0.3 ‰, then the maximum fractionation between the two most abundant ferric species $[\text{Fe}^{\text{III}}(\text{H}_2\text{O})_6]^{3+}$ and $[\text{Fe}^{\text{III}}(\text{H}_2\text{O})_5\text{Cl}]^{2+}$ in the LiCl ex-

periments cannot be more than $\sim 0.6\%$. Fractionation between the ferric-hydroxy and ferric-aquo complexes could perhaps be as much as $\sim 0.9\%$, given the smaller proportions of these species in our experiments (Table 2). Such large fractionation for ferric-hydroxy complexes seems unlikely, however, because Johnson et al. (2002a) measured a $\Delta_{\text{Fe(III)-Fe(II)}}$ of $+2.63 \pm 0.11\%$ at pH ~ 5.5 , where ferric speciation is 95% $[\text{Fe}^{\text{III}}(\text{H}_2\text{O})_5(\text{OH})]^{2+}$, suggesting that the $\Delta_{\text{Fe(III)-Fe(III)OH}}$ is $\sim 0.1\%$ or less.

4.3. Implications for Inorganic Fe Isotope Fractionation in Natural Systems

In oxygenated natural waters, inorganic Fe speciation is dominated by the octahedrally coordinated aquo or hydroxy complexes. Even in seawater, which contains ~ 0.5 mol/L Cl^- and 0.03 mol/L SO_4^{2-} , and 0.002 mol/L total CO_2 , dissolved ferrous speciation is dominated by $[\text{Fe}^{\text{II}}(\text{H}_2\text{O})_6]^{2+}$ and ferric speciation is dominated by $[\text{Fe}^{\text{III}}(\text{H}_2\text{O})_4(\text{OH})_2]^+$ ($>99\%$), $[\text{Fe}^{\text{III}}(\text{H}_2\text{O})_5(\text{OH})]^{2+}$, and $[\text{Fe}^{\text{III}}(\text{OH})_3]$ (e.g., Millero et al., 1995). As noted above, there is no evidence of significant Fe isotope fractionation between hexa-aquo Fe(III) and the soluble hydroxide species. Therefore, based on our current experiments, we predict that the inorganic equilibrium $\Delta_{\text{Fe(III)-Fe(II)}}$ should be constant at a given temperature in most dilute natural fluids, regardless of solution composition.

Bullen et al. (2001) determined a fractionation of $\sim +0.9\%$, between dissolved ferrous Fe and ferric oxyhydroxides along a natural hot springs flow path, as well as in precipitation experiments. Bullen et al. (2001) do not interpret their results to reflect isotopic fractionation between aqueous ferrous and ferric components, but between $[\text{Fe}^{\text{II}}(\text{H}_2\text{O})_6]^{2+}$ and $[\text{Fe}^{\text{II}}(\text{H}_2\text{O})_{6-n}(\text{OH})_n]^{2-n}$ species, arguing that rapid exchange involving the dissolved hydroxide species controls the isotopic fractionation that is observed. If true, then their results cannot reflect an equilibrium isotope factor because their arguments are fundamentally based on exchange kinetics (Johnson et al., 2003b).

Based on the isotope exchange kinetics determined in our experiments, relative to the moderate ferric hydroxide precipitation rates in the natural system and laboratory experiments of Bullen et al. (2001), we suggest that the $\sim +0.9\%$ fractionation between ferric oxyhydroxide and ferrous Fe reflect the effects of maintaining 100% isotopic equilibrium among aqueous Fe components during precipitation of ferric oxyhydroxide and/or kinetic isotope fractionation during precipitation of ferric Fe. For example, if complete isotope equilibrium is maintained between aqueous ferric and ferrous components, the apparent Fe isotope fractionation between ferric oxyhydroxide precipitate and ferrous Fe would be between about $+1.5$ to $+0.8\%$, depending on the aqueous ferrous/ferric ratio (Figs. 5 and 6), which overlaps the range measured by Bullen et al. (2001). Moreover, if the kinetic isotope fractionation of $+1.3\%$ between Fe(III) and ferric oxide precipitate measured by Skulan et al. (2002) is applicable to the experiments of Bullen et al. (2001), which were run on similar time scales, a net fractionation of $+1.5\%$ between ferric oxide and Fe(II) would be expected, and this lies within the range observed by Bullen et al. (2001). We therefore conclude that the results of Bullen et al. (2001) are likely to reflect kinetic effects, and

therefore are not directly comparable to the equilibrium fractionations determined in our study.

5. CONCLUSIONS

The experimentally determined equilibrium isotope fractionation between dissolved ferrous and ferric iron in inorganic solutions over a range of Cl^- concentrations, is constant, at a constant temperature. Isotopic fractionation between Fe(II) and Fe(III) in inorganic systems therefore should be independent of solution composition in most natural waters. The average measured $\Delta_{\text{Fe(III)-Fe(II)}}$ fractionation in our experiments is $+3.00 \pm 0.23\%$ at 22°C and $+3.57 \pm 0.38\%$ at 0°C . These fractionations are slightly different than those reported by Johnson et al. (2002a) because they are corrected for small errors in separation and recovery and for partial re-equilibration of ferrous and ferric iron during precipitation. However, rigorous assessment of the isotopic mass balance, as well as determination of the kinetics of exchange in solutions that are identical to those used for equilibrium fractionation determinations, confirm the validity of our initial work (Johnson et al., 2002a, 2003b), which has been recently questioned (Bullen et al., 2003). The measured fractionation between aqueous ferrous and ferric species is only about half of that predicted from spectroscopic data (Schauble et al., 2001).

The temperature dependence of Fe(III)-Fe(II) fractionation in dilute fluids can be described by the equation: $10^3 \ln \alpha_{\text{Fe(III)-Fe(II)}} = A * 10^6 / T^2 + B$ where $A = 0.334 \pm 0.032$ and $B = -0.88 \pm 0.38$ (T in $^\circ\text{K}$). At higher temperatures, for example 100°C , the expected $\Delta_{\text{Fe(III)-Fe(II)}}$ fractionation is estimated to be $+1.5 \pm 0.6\%$.

The kinetics of the ferrous-ferric isotopic exchange can be described by a second-order rate equation. Exchange kinetics are a complex function of chloride contents, although the equilibrium isotope fractionation factor is independent of $[\text{Cl}^-]$ over the range in our experiments. Exchange rates appear to be dominated by reaction between the $[\text{Fe}^{\text{III}}(\text{H}_2\text{O})_5(\text{OH})]^{2+}$ and $[\text{Fe}^{\text{II}}(\text{H}_2\text{O})_6]^{2+}$ species. Ferrous-ferric isotopic exchange rates were faster in HNO_3 than in HCl , which are interpreted to reflect higher concentrations of the $[\text{Fe}^{\text{III}}(\text{H}_2\text{O})_5(\text{OH})]^{2+}$ species. Exchange rates were faster in the LiCl solutions than the HCl solutions, possibly reflecting the effects of higher ionic strength, which should facilitate electron exchange.

Acknowledgments—This research was supported by funding from the National Science Foundation (EAR-0106614), the NASA Astrobiology Institute (NASA-Ames JRI NCC2-5449), and the Robert A. Welch Foundation, grant number B-1445. CMJ, BLB, and SAW are members of the NASA Astrobiology Institute associated with the Jet Propulsion Lab (JPL-1). PSB is an associate member of the Pennsylvania State University Astrobiology Research Center. We would like to thank Edwin Schauble, and two anonymous reviewers for their constructive reviews of this manuscript, and Associate Editor Simon Sheppard for his assistance.

Associate editor: S. M. F. Sheppard

REFERENCES

- Anbar A. D., Roe J. E., Barling J., and Nealon K. H. (2000) Nonbiological fractionation of iron isotopes. *Science* **288**, 126–128.

- Beard B. L. and Johnson C. M. (1999) High Precision iron isotope measurements of terrestrial and lunar material. *Geochim. Cosmochim. Acta* **63**, 1653–1660.
- Beard B. L., Johnson C. M., Cox L., Sun H., Neelson K. H., and Aguilari C. (1999) Iron isotope biosignatures. *Science* **285**, 1889–1892.
- Beard B. L., Johnson C. M., and Von Damm K. L. (2002) Iron isotope constraints on Fe cycling and mass balance in the oxygenated Earth. *Geochim. Cosmochim. Acta* **66**, A58 (abstr.).
- Beard B. L., Johnson C. M., Skulan J. L., Neelson K. H., Cox L., and Sun H. (2003a) Application of Fe isotopes to tracing the geochemical and biological cycling of Fe. *Chem. Geol.* **195**, 87–117.
- Beard B. L., Johnson C. M., Von Damm K. L., and Poulson R. L. (2003b) Iron isotope constraints on Fe cycling and mass balance in oxygenated Earth oceans. *Geology* **31**, 629–632.
- Brady G. W., Robein M. B., and Varimbi J. (1964) The structure of ferric chloride in neutral and acid solutions. *Inorg. Chem.* **3**, 1168–1173.
- Brunschwig B. S., Logan J., Newton M. D., and Sutin N. (1980) A semiclassical treatment of electron-exchange reactions. Application to the hexaquoiron(II)-hexaquoiron(III) system. *J. Chem. Soc.* **102**, 5798–5809.
- Brunschwig B. S., Creutz C., Macartney D. H., Sham T.-K., and Sutin N. (1982) The role of inner-sphere configuration changes in the electron exchange reactions of metal complexes. *Faraday Discussions Chem. Soc.* **74**, 113–127.
- Bullen T. D., White A. F., Childs C. W., Vivet D. V., and Schultz M. S. (2001) Demonstration of significant abiotic iron isotope fractionation in nature. *Geol.* **29**, 699–702.
- Bullen T. D., White A. F., and Childs C. W. (2003) Comment on “Isotopic fractionation between Fe(III) and Fe(II) in aqueous solutions” by Clark Johnson et al., [*Earth Planet. Sci. Lett.* **195**(2002),141–153]. *Earth Planet. Sci. Lett.* **206**, 229–232.
- Croal L. R., Johnson C. M., Beard B. L., Welch S., Poulson R., and Newman D. K. (2002) Development of an iron isotope biosignature for anaerobic photosynthetic Fe(II) oxidizing bacteria. *Geochim. Cosmochim. Acta* **66**, A157 (abstr.).
- Duncan J. F. and Cook G. B. (1968) *Iso. Chem.* Clarendon Press, Oxford.
- Eimer L., Medalia A. I., and Dodson R. W. (1952) Effect of oxygen on the ferrous-ferric exchange reaction. *J. Chem. Phys.* **20**, 743–744.
- Haim A. (1983) Mechanisms of electron transfer Reactions: the bridged activated complex. In *Progress in Inorganic Chemistry, and Appreciation of Henry Taube*, vol. **30** (ed. S. J. Lippard), pp. 273–357. John Wiley and Sons, New York.
- Hudis J. and Dodson R. W. (1956) Rate of ferrous-ferric exchange in D₂O. *J. Am. Chem. Soc.* **78**, 911–913.
- Hudis J. and Wahl A. C. (1953) The kinetics of the exchange reactions between iron (II) and the fluoride complexes of iron (III). *J. Am. Chem. Soc.* **75**, 4153–4158.
- Johnson C. M., Skulan J. L., Beard B. L., Sun H., Neelson K. H., and Braterman P. S. (2002a) Isotopic fractionation between Fe(III) and Fe(II) in aqueous solutions. *Earth Planet. Sci. Lett.* **195**, 141–153.
- Johnson C. M., Beard B. L., Welch S., Croal L., Newman D., and Neelson K. (2002b) Experimental constraints on Fe isotope fractionations during biogeochemical cycling of Fe. *Geochim. Cosmochim. Acta* **66**, A371 (abstr.).
- Johnson C. M., Beard B. L., Beukes N. J., Klein C., and O’Leary J. M. (2003a) Ancient geochemical cycling in the Earth as inferred from Fe isotope studies of banded iron formations from the Transvaal Craton. *Contrib. Mineral. Petrol.* **144**, 523–547.
- Johnson C. M., Beard B. L., Braterman P. S., and Welch S. A. (2003b) Reply to Comment on “Isotopic fractionation between Fe(III) and Fe(II) in aqueous solutions” by Thomas D. Bullen, Arthur F. White and Cyril W. Childs. *Earth Planet. Sci. Lett.* **206**, 233–236.
- Kanno H. and Hiraishi J. (1982) A raman study of aqueous solutions of ferric nitrate, ferrous chloride, and ferric chloride in the glassy state. *J. Ram. Spectros.* **12**, 224–227.
- Libby W. F. (1952) Theory of electron exchange reactions in aqueous solutions. *J. Phys. Chem.* **56**, 863–868.
- Luther G. W. III (1990) The frontier-molecular-orbital theory approach in geochemical processes. In *Aquatic Chemical Kinetics, Reaction Rates of Processes in Natural Waters* (ed. W. Stumm); pp.173–198. Wiley-Interscience publication.
- Magini R. and Radnai T. (1979) Xray diffraction study of ferric chloride solutions and hydrated melt. Analysis of the iron (III)-chloride complexes formation. *J. Chem. Phys.* **71**, 4225–4264.
- Matthews A., Zhu X.-K., and O’Nions K. (2001) Kinetic iron stable isotope fractionation between iron (-II) and (-III) complexes in solution. *Earth Planet. Sci. Lett.* **192**, 81–92.
- Millero F. J., Yao W., and Aicher J. (1995) The speciation of Fe(II) and Fe(III) in natural waters. *Mar. Chem.* **50**, 21–39.
- Parkhurst D. L. (1995) User’s guide to PHREEQC-A computer program for speciation, reaction-path, advective-transport, and inverse geochemical calculations. Water-Resources Investigation Report 95-4227. U.S. Geological Survey, Lakewood CO. pp. 143.
- Polyakov V. B. (1997) Equilibrium fractionation of the iron isotopes: Estimation from Mössbauer spectroscopy data. *Geochim. Cosmochim. Acta* **61**, 4213–4217.
- Polyakov V. B. and Mineev S. D. (2000) The use of Mössbauer spectroscopy in stable isotope geochemistry. *Geochim. Cosmochim. Acta* **64**, 849–865.
- Poulson R., Beard B. L., Pierson B. K., and Johnson C. M. (2002) Iron isotope variations at Chocolate Pots Hot Springs, Yellowstone National Park—Modern analog for ancient geochemical cycling. *Astrobiol. Sci. Conf.* **2002**, NASA AMES Research Center, Moffet Field CA. April 8–11. 2002.
- Schauble E. A., Rossman G. R., and Taylor H. P. Jr. (2001) Theoretical estimates of equilibrium Fe-isotope fractionations from vibrational spectroscopy. *Geochim. Cosmochim. Acta* **65**, 2487–2497.
- Sharma S. K. (1974) Raman study of ferric chloride solutions and hydrated melts. *J. Chem. Phys.* **60**, 1368–1375.
- Sharma S. K., Sehgal V. N., Bami H. L., and Sharma S. D. (1975) Raman study of the structure of ferric chloride in frozen aqueous solutions. *J. Inorg. Nuc. Chem.* **37**, 2417–2419.
- Silverman J. and Dodson R. W. (1952) The exchange reaction between the two oxidation states of iron in acid solution. *J. Phys. Chem.* **56**, 846–852.
- Skulan J. L., Beard B. L., and Johnson C. M. (2002) Kinetic and equilibrium Fe isotope fractionation between aqueous Fe(III) and hematite. *Geochim. Cosmochim. Acta* **66**, 2995–3015.
- Stookey L. L. (1970) Ferrozine—a new spectrophotometric reagent for iron. *Anal. Chem.* **42**, 779–781.
- Sutin N. (1983) Theory of electron transfer reaction: Insights and Hindsights. In *Progress in Inorganic Chemistry, and Appreciation of Henry Taube* vol. **30** (ed. S. J. Lippard), pp. 441–498. John Wiley and Sons, New York.
- Sutin N. (1986) Theory of Electron Transfer Reactions. In *Inorganic Reactions and Methods* Vol. **15** (ed. J. J. Zuckerman), pp. 16–47. VCH Publishers, Inc., Deerfield Beach, FL.
- Sutin N. (1999) Electron transfer reactions in solution: A historical perspective. In *Electron Transfer—from Isolated Molecules to Biomolecules, part one*. (eds. J. Jortner and M. Bixon) *Advances in Chemical Physics*, Vol **106**, pp. 7–33. John Wiley and Sons, New York.
- Sutin N., Rowley J. K., and Dodson R. W. (1961) Chloride complexes of iron (III) ions and the kinetics of the chloride-catalyzed exchange reaction between iron (II) and iron (III) in light and heavy water. *J. Phys. Chem.* **65**, 1248–1252.
- Taube H. (1984) Electron transfer between metal complexes: Retrospective. *Science* **226**, 1028–1036.
- Urey H. C. (1947) The thermodynamic properties of isotopic substances. *J. Chem. Soc. (London)*. 562–581.
- Wehrli B. (1990) Redox reactions of metal ions at mineral surfaces. In *Aquatic Chemical Kinetics, Reaction Rates of Processes in Natural Waters* (ed. W. Stumm), pp. 311–336. Wiley-Interscience publication, New York.
- Zhu X. K., O’Nions R. K., Guo Y. L., and Reynolds B. C. (2000) Secular variation of iron isotopes in North Atlantic deep water. *Science* **287**, 2000–2002.
- Zhu X. K., Guo Y., Williams R. J. P., O’Nions R. K., Matthews A., Belshaw N. S., Canters G. W., Waal E. C., Weser U., Burgess B. K.,

and Salvato B. (2002) Mass fractionation processes of transition metal isotopes. *Earth Planet. Sci. Lett.* **200**, 47–62.

APPENDIX

A.1. Determination of first-order rate coefficients

We model the overall exchange as second-order, but the rate of ferric-ferrous isotopic exchange can also be modeled as a first order reaction with respect to either ferrous or ferric iron. Substituting the extent of isotopic exchange (F, Eqn. 5) into the general rate Eqn. 6 for a first-order reaction gives:

$$\ln(1 - F) = -k_1 t \quad (17)$$

where k_1 is the first-order rate constant, and t is time in seconds (Table A.1). The trends observed for the reactivity of isotope exchange in the different solutions are similar whether the reaction is considered to be first order with respect to ferrous or ferric Fe or second order overall.

The first-order rate coefficients calculated in our exchange experiments can be related to previous determinations of ferrous-ferric exchange rate (e.g., Silverman and Dodson, 1952) assuming:

$$k_{(\text{obs})} = k_{(\text{FeII})}[\text{Fe(III)}] \text{ or } k_{(\text{obs})} = k_{(\text{FeIII})}[\text{Fe(II)}] \quad (18)$$

where $k_{(\text{obs})}$ is the first-order rate coefficient obtained from a linear fit of $-\ln(1-F)$. Substituting values for $k_{(\text{obs})}$ and $[\text{Fe}]$ for our experimental conditions yields values for $k_{(\text{FeII})}$ or $k_{(\text{FeIII})}$ of approximately 300 to 3000 $\text{M}\cdot\text{s}^{-1}$, which are comparable to the exchange rate coefficient of $\sim 1000 \text{ M}\cdot\text{s}^{-1}$ calculated for electron exchange between $[\text{Fe}^{\text{II}}(\text{H}_2\text{O})_6]^{2+}$ and $[\text{Fe}^{\text{III}}(\text{H}_2\text{O})_5(\text{OH})]^{2+}$ (see Table 8; Silverman and Dodson, 1952; Hudis and Wahl, 1953; Sutin et al., 1961).

Table A1. First-order rate constants based on ferrous data, predicted F values at $t = 1$ second.

Experiment	Rate k_1	F at $t = 1$ sec
HNO ₃ 22°C	-0.110 ± 0.020	0.102
HCl 22°C	-0.046 ± 0.003	0.047
LiCl 22°C	-0.052 ± 0.005	0.051
HNO ₃ 0°C	-0.011 ± 0.002	0.011
HCl 0°C	-0.009 ± 0.001	0.010
LiCl 0°C	-0.013 ± 0.001	0.013

It is important to note that estimates for the extent of isotopic exchange that could occur during species separation by ferric oxyhydroxide precipitation are considerably less if the exchange reaction is modeled as first order. Estimates of the percent exchange based on the uncorrected F values are ~ 5 to 10% at 22°C and $\sim 1\%$ at 0°C using first-order rate equation, compared to ~ 30 to 40% at 22°C and $\sim 10\%$ at 0°C assuming second order exchange kinetics. Using these exchange rates, we can estimate uncertainties in the measured $\Delta_{\text{Fe(III)-Fe(II)}}$ due to partial re-equilibration if overall isotopic exchange is first order. Assuming an arbitrary $\Delta_{\text{Fe(III)-Fe(oxide)}}$ of +0.5 ‰, then the maximum correction for $\Delta_{\text{Fe(III)-Fe(II)}}$ is ~ 0.08 ‰, indicating that our measured ferric-ferrous fractionation will be essentially identical to the true fractionation factor if corrections using first-order rate equations are appropriate.